NASA Contractor Report 187628
ICASE Report No. 91–71

ICASE

THE STABILITY OF NUMERICAL BOUNDARY TREATMENTS FOR COMPACT HIGH-ORDER FINITE-DIFFERENCE SCHEMES

Mark H. Carpenter
David Gottlieb
Saul Abarbanel

Contract No. NAS1–18605
September 1991

Institute for Computer Applications in Science and Engineering
NASA Langley Research Center
Hampton, Virginia 23665–5225

Operated by the Universities Space Research Association

National Aeronautics and
Space Administration

Langley Research Center
Hampton, Virginia 23665-5225

THE STABILITY OF NUMERICAL BOUNDARY TREATMENTS FOR COMPACT HIGH-ORDER FINITE-DIFFERENCE SCHEMES

Mark H. Carpenter
NASA Langley Research Center, Hampton, VA 23665

David Gottlieb[1]
Brown University, Providence, RI 02192

and

Saul Abarbanel
Tel-Aviv University, Tel-Aviv, ISRAEL

ABSTRACT

The stability characteristics of various compact fourth- and sixth-order spatial operators are assessed using the theory of Gustafsson, Kreiss and Sundstrom (G-K-S) for the semi-discrete Initial Boundary Value Problem (IBVP). These results are then generalized to the fully discrete case using a recently developed theory of Kreiss. In all cases, favorable comparisons are obtained between G-K-S theory, eigenvalue determination, and numerical simulation. The conventional definition of stability is then sharpened to include only those spatial discretizations that are asymptotically stable (bounded, Left Half-Plane eigenvalues). It is shown that many of the higher-order schemes which are G-K-S stable are not asymptotically stable. A series of compact fourth- and sixth-order schemes, which are both asymptotically and G-K-S stable for the scalar case, are then developed.

[1]This research was supported by the National Aeronautics and Space Administration under NASA Contract No. NAS1-18605 while the second and third authors were in residence at the Institute for Computer Applications in Science and Engineering (ICASE), NASA Langley Research Center, Hampton, VA 23665.

1. INTRODUCTION

Recently, higher-order numerical methods have seen increasing use in the Direct Numerical Simulation (DNS) of the Navier-Stokes equations. Although they do not have the spatial resolution of Spectral methods, they offer significant increases in accuracy over conventional second-order methods. They can be used on any smooth grid, and do not have an overly restrictive CFL dependence as compared with the $O(N^{-2})$ CFL dependence observed in some Spectral methods on finite domains. In addition, they are generally more robust and less costly than Spectral methods. The issue of the relative cost of higher-order schemes (accuracy weighted against physical and numerical cost) is a very complex issue, ultimately depending on what features of the solution are sought and how accurately they must be resolved. In any event, the further development of the underlying stability theory of these schemes is important.

The state of higher-order temporal discretizations is well developed and relies greatly on the existing Ordinary Differential Equation (ODE) literature. Higher-order spatial discretizations are well documented in the literature, as well. For example, entire classes of centered explicit spatial schemes are described in the text of Kopal [1]. In practice, compact schemes (methods where both the solution and its derivatives are treated as unknowns and are solved for simultaneously) are more accurate than optimal explicit schemes (nth order schemes involving n+1 grid-points), and have gained much attention recently for use in DNS. The fundamental ideas of compact schemes as well as derivation techniques can be found in the work of Vichnevetsky [2], and will not be pursued in this work. The primary difficulty in using higher-order schemes is finding stable boundary schemes that preserve their formal accuracy. It is well known that for a hyperbolic system to preserve formal spatial accuracy, an $(N)^{th}$ order inner-scheme must be closed with at least an $(N-1)^{th}$ order boundary scheme [3]. To date, many higher-order inner-schemes are used with lower-order boundary schemes, because no stable higher-order formulations are known. The formal accuracy of these formulations is thus reduced to one order more than the Boundary Condition (BC) accuracy, and it is questionable whether the additional work incurred in the higher-order inner-scheme is justified.

Determining the numerical stability of a fully discrete approximation for a linear hyperbolic partial differential equation is a difficult task. For the "Cauchy Problem" on an infinite domain $(-\infty, \infty)$, standard techniques based on Fourier methods generally provide the necessary conditions for stability of the numerical scheme. For the Initial-Boundary-Value Problem (IBVP) on the semi-infinite domain $[0, \infty)$, or the finite domain [-1,1], *Fourier* techniques are not straight forward to apply and do not provide sufficient conditions for numerical stability. To address these issues, Osher [4] and Kreiss [5], and later Gustafsson et

al. [6], developed stability analysis techniques based on normal mode analysis. Their work (generally referred to as G-K-S stability theory) established conditions that the inner and boundary schemes must satisfy, to ensure stability. The G-K-S theory states that hyperbolic systems are assured stability if no eigenvalues or generalized eigenvalues exist for the IBVP. Trefethen [7] further clarified the physical meaning of the G-K-S condition by noting that the concept of stability at a boundary could be related to the group velocity of the boundary scheme, specifically, whether it is carrying energy into or out of the numerical domain.

One of the weak points of fully discrete G-K-S theory has been the great complexity in applying it to higher-order numerical schemes. Raising the spatial or temporal accuracy generally increases the complexity of the stability polynomials (the order increases, giving rise to more roots) which govern the stability of the numerical approximation. In multi-stage time discretization schemes (e.g. Runge-Kutta schemes with three or more stages), where boundary conditions must be applied at intermediate levels, the stability polynomials that must be tested at each boundary are nearly insurmountable using analytic techniques. One can greatly simplify the analysis by addressing the semi-discrete problem as a method-of-lines IBVP, rather than the fully discrete problem. The underlying G-K-S theory for the semi-discrete problem was initially developed by Strikwerda [8]. He showed that by discretizing space and leaving time continuous, the necessary and sufficient conditions for method-of-lines IBVP stability are analogous to those governing the stability of the fully discrete case.

The precise connection between the semi-discrete stability bounds and those obtained in the fully discrete analysis is not always straight forward. Recently, however, Kreiss et al. [9] have shown that under very weak conditions, stability of the semi-discrete approximation infers stability in the fully discrete approximation if specific Runge-Kutta time marching schemes are used. Therefore, one can rely on the semi-discrete G-K-S theory to assess the stability with R-K integration, of various higher-order spatial discretization operators, thus simplifying the calculations considerably.

The emphasis of this work is to apply semi-discrete G-K-S theory to several higher-order spatial operators for the IBVP. Since compact methods naturally lend themselves to fewer implementational difficulties at the boundaries, they will be the primary focus. Stable boundary formulations which preserve the formal accuracy of the inner-scheme will be presented for spatial derivative operators of up to sixth-order.

2. MODEL EQUATION FOR IBVP

Under the assumption of locally frozen coefficients, the equations governing conservation of mass, momentum and energy in one spatial dimension can be transformed into a system

of hyperbolic equations, having the form:

$$\frac{\partial U}{\partial t} = A\frac{\partial U}{\partial x} + F;\ \ x \geq 0,\ \ t \geq 0 \tag{1}$$

where "A" is a diagonal matrix with real eigenvalues, F is a source term, and boundary and initial data are supplied in the form

$$U^I(0,t) + TU^{II}(0,t) = g(t),\ \ U(x,0) = f(x) \tag{2}$$

where T is a matrix describing the boundary conditions, and A has been divided into its right- and left-going characteristics to determine the boundary conditions. The problem is said to be well-posed if the solution U(x,t) depends smoothly on the initial and boundary data. Our focus in this work will be on the scalar form of eqn (1-2), where the matrix "A" is a negative real constant "a" and with the source term F = 0. This simplification can be justified since stability of a numerical scheme on the scalar equation implies stability of the system if boundary conditions are imposed in a characteristic form (ex. see Gottlieb et al. [10]). A further necessary modification is that the semi-infinite spatial domain must be truncated to a finite domain. For simplicity, we shall assume that the physical domain is confined to the interval $0 \leq x \leq 1$ for all times.

3. SEMI-DISCRETIZATION

In this work, the numerical discretization of eqn (1) will be accomplished by two separate and independent steps. The spatial derivatives will first be approximated with appropriate formulas, leaving what is generally referred to as a semi-discretization. The numerical solution will then be advanced in time in a Method-of-Lines approach, using a stable temporal scheme. We begin by dividing the continuous domain [0,1] into N uniform intervals of width Δx where $N\Delta x = 1$. The continuous derivative U_x is then replaced with a finite-difference representation involving the functional values U_j at the discrete points. A system of ODE's results having the form

$$\frac{dV_j}{dt} = M^+V_j\ \ j = 0,\ \ldots,N \tag{3}$$

where

$$M^+V_j = \sum_{k=-L_j}^{R_j} a\ m_j^k V_{j+k} \tag{4}$$

and "L" and "R" are the width of the stencil extending to the left and right of grid-point j, respectively. Note that m_j^k, L_j and R_j are functions of "j" since there is no reason to

assume that the same stencil will be used at each grid-point. For example, consider the case where the same spatial stencil is used at every interior grid-point in the domain. We, therefore, choose a particular $L_j = L$ and $R_j = R$. (Obviously, the choice of L, R, and m_j^k should coincide with a scheme that is stable for the Cauchy problem on the infinite domain). This scheme can only be used for $L < j < N - R$ without the stencil protruding through the boundary. Thus, exactly L + R additional formulas have to be defined near the boundaries. Since there is only one physical boundary condition, L + R - 1 of the schemes are strictly numerically motivated. These schemes are generally referred to as numerical boundary schemes (NBS).

Noting that the physical boundary condition g(t) will be imposed at the grid-point j=0, eqn (3) can be rewritten as

$$\frac{dV_j}{dt} = MV_j + B_j g(t);\ \ j = 1, \ldots, N \tag{5}$$

where M is an N x N matrix, and B_j is a vector of dimension N, describing the dependence of the "j^{th}" scheme on the boundary data. The matrix M usually is diagonal of order L + R + 1 for most explicit methods, but can in general be full. With little loss of generality, g(t) can be chosen to be zero. The exact solution of the semi-discretization described by eqn (5) for homogeneous boundary data becomes

$$V_j(t) = f(x_j)\exp^{Mt};\ \ j = 1, \ldots, N. \tag{6}$$

Note that all the boundary information is incorporated directly into the matrix M. and that the stability of the numerical scheme depends directly on the properties of the matrix, not just on what spatial discretization was chosen for the inner-scheme.

It is instructive to clarify these points involving boundary closures with examples of an explicit and an implicit spatial scheme. We choose to concentrate on schemes having at least fourth-order spatial accuracy since most of the difficulties associated with high-order stencils are not observed with second-order schemes. The first is an explicit 5-point scheme reported by Gary [11], and later shown by Strikwerda [8] to be G-K-S stable. The scheme is uniformly fourth-order in space. The spatial discretization is accomplished with the stencils

$$\begin{aligned}
\frac{\partial V_0}{\partial x} &= \frac{1}{12\Delta x}(-25V_0 + 48V_1 - 36V_2 + 16V_3 - 3V_4) \\
\frac{\partial V_1}{\partial x} &= \frac{1}{12\Delta x}(-3V_0 - 10V_1 + 18V_2 - 6V_3 + V_4) \\
\frac{\partial V_j}{\partial x} &= \frac{1}{12\Delta x}(V_{j-2} - 8V_{j-1} + 8V_{j+1} - V_{j+2}); \qquad j = 2, \ldots, N-2 \\
\frac{\partial V_{N-1}}{\partial x} &= \frac{1}{12\Delta x}(-V_{N-4} + 6V_{N-3} - 18V_{N-2} + 10V_{N-1} + 3V_N) \\
\frac{\partial V_N}{\partial x} &= \frac{1}{12\Delta x}(3V_{N-4} - 16V_{N-3} + 36V_{N-2} - 48V_{N-1} + 25V_N).
\end{aligned} \tag{7}$$

The terms in eqn (3) take the form

$$V^+ = \begin{bmatrix} V_0 \\ V_1 \\ V_2 \\ V_3 \\ \cdot \\ \cdot \\ \cdot \\ V_{N-2} \\ V_{N-1} \\ V_N \end{bmatrix}, \quad \hat{M}^+ = \begin{bmatrix} -25 & 48 & -36 & 16 & -3 & & & & & \\ -3 & -10 & 18 & -6 & 1 & & & & & \\ 1 & -8 & 0 & 8 & -1 & & & & 0 & \\ & 1 & -8 & 0 & 8 & -1 & & & & \\ & & \cdot & \cdot & \cdot & \cdot & \cdot & & & \\ & & & \cdot & \cdot & \cdot & \cdot & \cdot & & \\ & & & & \cdot & \cdot & \cdot & \cdot & \cdot & \\ & & & & & 1 & -8 & 0 & 8 & -1 \\ & & 0 & & & -1 & 6 & -18 & 10 & 3 \\ & & & & & 3 & -16 & 36 & -48 & 25 \end{bmatrix} \tag{8}$$

where $M^+ = \frac{a}{12\Delta x}\hat{M}^+$. Note that four NBS's are required to close the numerical scheme, of which only one will be overwritten by a physical boundary condition. Accounting for the boundary condition at the grid-point j=0 in eqn (8), results in expressions for eqn (5) of the form

$$V = \begin{bmatrix} V_1 \\ V_2 \\ V_3 \\ \cdot \\ \cdot \\ \cdot \\ V_{N-2} \\ V_{N-1} \\ V_N \end{bmatrix}, \quad \hat{M} = \begin{bmatrix} -10 & 18 & -6 & 1 & & & & & \\ -8 & 0 & 8 & -1 & & & & 0 & \\ 1 & -8 & 0 & 8 & -1 & & & & \\ & \cdot & \cdot & \cdot & \cdot & \cdot & & & \\ & & \cdot & \cdot & \cdot & \cdot & \cdot & & \\ & & & \cdot & \cdot & \cdot & \cdot & \cdot & \\ & & & & 1 & -8 & 0 & 8 & -1 \\ & 0 & & & -1 & 6 & -18 & 10 & 3 \\ & & & & 3 & -16 & 36 & -48 & 25 \end{bmatrix}, \quad \hat{B} = \begin{bmatrix} -3 \\ 1 \\ 0 \\ \cdot \\ \cdot \\ \cdot \\ 0 \\ 0 \\ 0 \end{bmatrix} \tag{9}$$

where $M = \frac{a}{12\Delta x}\hat{M}$ and $B = \frac{a}{12\Delta x}\hat{B}$. It is evident that the matrix M is the N x N submatrix of the matrix M^+, corresponding to $1 \leq i, j \leq N$.

The implicit fourth-order example is that of a compact discretization in which the numerical approximation to $\frac{\partial U_j}{\partial x}$ is made in the following form

$$\begin{aligned} \frac{\partial V_0}{\partial x} + 3\frac{\partial V_1}{\partial x} &= \frac{1}{6\Delta x}(-17V_0 + 9V_1 + 9V_2 - V_3) \\ \frac{\partial V_{j-1}}{\partial x} + 4\frac{\partial V_j}{\partial x} + \frac{\partial V_{j+1}}{\partial x} &= \frac{1}{\Delta x}(-3V_{j-1} + 3V_{j+1}) \\ \frac{\partial V_{N-1}}{\partial x} + \frac{\partial V_N}{\partial x} &= \frac{1}{6\Delta x}(V_{N-3} - 9V_{N-2} - 9V_{N-1} + 17V_N). \end{aligned} \tag{10}$$

Noting the structure of the spatial operator and the fact that $\frac{\partial V_j}{\partial t} = a\frac{\partial V_j}{\partial x}$, for this scheme, eqn (3) is often rearranged into the form

$$M_1^+ \frac{dV_j}{dt} = M_2^+ V_j; \;\; j = 0, \ldots, N \tag{11}$$

where $M^+ = (M_1^+)^{-1} M_2^+$. The resulting matrix expression becomes

$$V^+ = \begin{bmatrix} V_0 \\ V_1 \\ . \\ . \\ . \\ V_{N-1} \\ V_N \end{bmatrix}, \qquad M_1^+ = \begin{bmatrix} 6 & 18 & & & & & \\ 1 & 4 & 1 & & & 0 & \\ & . & . & . & & & \\ & & . & . & . & & \\ & & & . & . & . & \\ & 0 & & & 1 & 4 & 1 \\ & & & & & 18 & 6 \end{bmatrix},$$

$$\hat{M}_2^+ = \begin{bmatrix} -17 & 9 & 9 & -1 & & & \\ -3 & 0 & 3 & & & 0 & \\ & . & . & . & & & \\ & & . & . & . & & \\ & & & . & . & . & \\ & 0 & & & -3 & 0 & 3 \\ & & & 1 & -9 & -9 & 17 \end{bmatrix} \tag{12}$$

where $M_2^+ = \frac{a}{\Delta x} \hat{M}_2$. Imposing the boundary information at grid-point j=0 reduces the matrix by one order and yields matrix equations of the form

$$V = \begin{bmatrix} V_1 \\ V_2 \\ . \\ . \\ . \\ V_{N-1} \\ V_N \end{bmatrix}, \qquad M_1 = \begin{bmatrix} 6 & 6 & & & & & \\ 1 & 4 & 1 & & & 0 & \\ & . & . & . & & & \\ & & . & . & . & & \\ & & & . & . & . & \\ & 0 & & & 1 & 4 & 1 \\ & & & & & 18 & 6 \end{bmatrix},$$

$$\hat{M}_2 = \begin{bmatrix} -1 & 9 & 9 & & & & \\ -3 & 0 & 3 & & & 0 & \\ & . & . & . & & & \\ & & . & . & . & & \\ & & & . & . & . & \\ & 0 & & & -3 & 0 & 3 \\ & & & 1 & -9 & -9 & 17 \end{bmatrix}, \qquad \hat{B}_2 = \begin{bmatrix} -1 \\ 0 \\ . \\ . \\ . \\ 0 \\ 0 \end{bmatrix} \tag{13}$$

where $B_2 = \frac{a}{\Delta x} \hat{B}_2$. Note that because a matrix multiplication was involved in determining the spatial operator for grid-points $1 \leq j \leq N$, matrix M is not a simple submatrix of matrix M^+ as it was with the explicit scheme. The spatial operator described by eqn (13) is referred to as being compact because both M_1 and M_2 only involve three grid-points (except near the boundary in M_2). Because of this compactness, L = R = 1 , and only two NBS must be defined (one of which includes, but is not replaced by, the physical boundary condition).

Expressing this algorithm in the form of eqn (5) yields

$$M = M_1^{-1} M_2, \quad B = M_1^{-1} B_2. \tag{14}$$

It is apparent that while the algorithm is implementationally compact, the resulting M is a full N x N matrix.

Working with the scalar form of eqn (1), with the boundary conditions posed at x=0, has allowed us to simplify the semi-discretization defined by eqn (3) to that of eqn (5). Note that if the governing equation would have been $U_t + aU_x = F$ with boundary data at x = 1, the two previously mentioned schemes could have easily accommodated this change and still produced a stable algorithm. For a system of hyperbolic equations with variable coefficients, one does not know a priori the sign of the eigenvalues of the matrix A in eqn (1). Therefore, the solution is advanced in time for j=0,N, followed by a characteristic decomposition in which the physical boundary conditions are imposed at either j=0 or j=N such that the resulting system is well-posed. This requirement imposes a constraint on the class of allowable matrices M^+ which can be conveniently used to obtain stable discretizations. Only central-difference schemes have this desirable feature; that of being stable for $a > 0$, or $a < 0$. Assuming that a central-difference operator is used throughout the interior domain, then eqn (4) requires that R = L NBS's be defined at each boundary. The structure of these NBS's must be such that the resulting scheme be stable for either the inflow (a < 0; j=1,N) or the outflow (a > 0; j=0,N-1). This can only be accomplished if the same methodology is used to derive the NBS's at each end of the domain. Therefore, the NBS's at each respective boundary, are asymmetric mirror images of each other. The resulting matrix M^+ has the following property

$$M^+ = -PM^+P \tag{15}$$

where P is the permutation operator defined by $p_{i,j} = 0, 0 \leq i,j \leq N$, for $i \neq N - j$, and $p_{i,j} = 1, 0 \leq i,j \leq N$, for $i = N - j$. Note that PP = I, the identity matrix. The matrix M is, therefore, the N x N submatrix of M^+.

We now have a well defined class of spatial operators which are acceptable for our purposes. They are high-order central difference schemes with boundary implementations which are imposed asymmetrically. For future reference, we shall define a convenient nomenclature to describe these matrices. The matrix M^+ shall be described as $(NBS_1, \cdots, NBS_L - CD - NBS_R, \cdots NBS_N)$, where "CD" is the order of the central difference operator used in the interior, and NBS_j is the order of the NBS used to close the scheme at the points next to the boundary. For example, the explicit uniformly fourth-order scheme represented by matrix eqn (8) is denoted by the nomenclature (4,4-4-4,4), where the "-4-" denotes the

inner-scheme being approximated with a fourth-order stencil, and the symmetric "4,4" denotes fourth-order stencils at j=0,1, and j=N-1,N. The three-point compact scheme described by eqn (12) is denoted (4-4-4). Again, the "-4-" refers to the inner-scheme accuracy, and the symmetric "4"s indicate closure on the boundaries of fourth-order accuracy. There is no ambiguity in the nomenclature between the compact and explicit schemes, since only the compact scheme can retain fourth-order inner accuracy with one NBS at each boundary.

4. STABILITY OF THE IBVP

The eigenvalues of matrix M from eqn (5), resulting from higher-order finite-difference approximations to U_x, tend to align along the imaginary axis in complex conjugate pairs. To time advance eqn (5) efficiently, the time discretization algorithm should include in its stability domain a large portion of the imaginary axis. Conventional Runge-Kutta (R-K) time advancement algorithms of third- or fourth-order are well suited for semi-discretizations of hyperbolic equations, and are the only method considered in this study. In particular, the standard fourth-order method of Kutta (ex. see Gear [12]) will be used in this study because of the 1) fourth-order non-linear accuracy, 2) the large stability envelope, and 3) the low storage requirements.

It is desired to know whether a given higher-order spatial discretization is stable for this time advancement scheme. Using conventional G-K-S theory for the fully discrete IBVP for fourth-order R-K time, and second-order space discretization would involve polynomials of eighth-order in κ to solve at the boundaries. Closed form solutions would be difficult to obtain under these circumstances, and would get more complicated with increasing spatial accuracy. The stability analysis can be greatly simplified by relying on three fundamental theorems of stability analysis which are valid under the conditions proposed in this study. We will discuss each briefly, but for further clarification suggest consulting the original works. The essential elements of the theorems forming the basis of this work are:

Theorem 1: G-K-S theory (fully discrete [6] or semi-discrete [8]) asserts that to show stability for the finite domain problem, it is sufficient to show that the inner-scheme is Cauchy stable on $(-\infty, \infty)$, and that each of the two quarter-plane problems is stable using normal mode analysis. Thus, the stability of the finite-domain problem is broken into the summation of three simpler problems.

Theorem 2: For each quarter plane problem arising in theorem 1, a necessary and sufficient condition for stability of the initial boundary value problem is that there exist no eigensolution. This theorem is true for either the fully-discrete case [6], or the semi-discrete case [8].

The algebraic complexity involved in showing stability of the IBVP is dramatically reduced in the semi-discrete case, since time remains continuous. Ultimately, numerical stability is a fully-discrete concept, and a connection between the semi- and fully-discrete stability must be used. The third theorem provides this connection.

Theorem 3: Under mild restrictions [9], if a semi-discrete approximation is stable in a generalized sense and a Runge-Kutta method which is locally stable is used to time march the semi-discretization, the resulting totally discrete approximation is stable in the same sense so long as the stability region of the R-K method encompasses the norm of the semi-discretization.

It should be noted [9] that the stability definitions used in the first two theorems (G-K-S stability) are different than that of the third (generalized stability). The first two theorems rely on G-K-S stability (sometimes referred to as the Kreiss condition) in the semi- or fully-discrete case. At least two different definitions of G-K-S stability are encountered in the cumulative works on G-K-S analysis. They are:

Definition 1: The IBVP is stable if for $\eta > \eta_o$, the solutions of eqn (1) with homogeneous initial data satisfy

$$|\hat{U}(0,S)|^2 + (\eta - \eta_o)^2 \|\hat{U}(.,S)\|^2 \leq K(|\hat{g}|^2 + \|\hat{F}(.,S)\|^2) \tag{16}$$

where η_o and K are universal constants, and the $\hat{}$ denotes the Laplace transformed variables.

Definition 2: The IBVP is stable if for $\eta > \eta_o$, the solutions of eqn (1) with homogeneous initial data and g = 0 satisfy

$$(\eta - \eta_o)\|\hat{U}(.,S)\| \leq K(\|\hat{F}(.,S)\|). \tag{17}$$

Both of these definitions can be related to what is often referred to as Lax stability, which is the numerical equivalent to an energy estimate satisfied by the discrete form of eqn (1,2).

Theorem 3 relies on a different definition of stability that can be expressed as

Definition 3: The IBVP is stable if for homogeneous boundary data (g=0) an estimate of the form

$$\|U(.,t)\| = K \exp^{\alpha(t-t_o)}(\|U(.,t_o)\| + \int_o^t \|F(.,\tau)\| d\tau). \tag{18}$$

Definition 2 is the most restrictive of the three conditions, but it has been conjectured by Kreiss [9] that Definition 2 and 3 are equivalent. The subtle differences between these definitions of stability will not affect the conclusions in this work, and the terms G-K-S

stability and Lax-stability shall be used interchangeably. We now describe in some detail the implications of the three Theorems.

The chief difficulty in stability analysis is not which definition is chosen, but rather applying that definition to practical numerical methods and obtaining a stability bound. Since Fourier methods are not well suited on the finite domain, stability analysis can be carried out by energy methods or by normal mode analysis. Energy methods are, in general, very difficult to perform on high-order schemes. The modal relationships are simple to define but analytic solutions are often intractable.

Theorem 1 describes how G-K-S analysis can be used to augment finite domain modal analysis. The original finite domain modal analysis is broken into the analysis of three equivalent, yet simpler modal problems. Assuming that a Cauchy stable scheme is used for the interior grid-points, the inner-scheme is tested for stability at each boundary in a semi-infinite spatial domain. In so doing, the stability of each boundary is independent of the influence from the other boundary. Stability of the two boundary problems implies stability of the finite domain numerical method. In addition, Theorem 1 provides a "perturbation test" for "generalized eigensolutions." The test establishes the stability of certain borderline cases in normal mode analysis.

To fully appreciate the power of G-K-S analysis, a normal mode analysis of the fourth-order compact scheme (4-4-4) described by eqn (13) is presented for the coupled finite domain problem. We proceed by assuming that the semi-discrete problem defined in eqn (11) has a solution of the form

$$V_j(t) = \exp^{St} \phi_j \tag{19}$$

where "S" are the eigenvalues of the matrix $M_1^{+-1} M_2^+$. Substitution into eqn (11) yields the generalized eigenvalue problem

$$M_1^+ S V_j = M_2^+ V \tag{20}$$

(for which we have assumed g(t) = 0), and the resolvent equation provided by the inner-scheme is

$$(\phi_{j-1} + 4\phi_j + \phi_{j+1})\hat{S} = 3(-\phi_{j-1} + \phi_{j+1}) \;\; j = 2, \ldots, N-1 \tag{21}$$

where $\hat{S} = \frac{\Delta x}{a} S$. It is apparent that $\phi_j = \phi_o \kappa^j$ will satisfy this expression, yielding the following equation for the eigenvalues

$$(\frac{1}{\kappa} + 4 + \kappa)\hat{S} = 3(\frac{-1}{\kappa} + \kappa). \tag{22}$$

This is a quadratic expression in κ, and there will, in general, be two solutions which will satisfy eqn (22). The eigenvectors are, therefore, of the form $\phi_j = C_1\kappa_1{}^j + C_2\kappa_2{}^j$. Simple manipulations show the two roots are related by

$$\kappa_1 = \kappa, \;\; \kappa_2 = \frac{-2-\kappa}{2\kappa+1} \tag{23}$$

and

$$\phi_j = C_1\kappa^j + C_2\left(\frac{-2-\kappa}{2\kappa+1}\right)^j. \tag{24}$$

We note that if $\kappa = a + ib$, then

$$|\kappa_1| = a^2 + b^2, \;\; |\kappa_2| = \frac{b^2 + (a+2)^2}{(2b)^2 + (2a+2)^2} \tag{25}$$

and $|\kappa_1| \geq 1$ implies $|\kappa_2| \leq 1$. Thus, each κ is dominant near one of the boundaries and its influence decays monotonically with increasing distance from that boundary. The form of C_1 and C_2 must be determined from the boundary conditions at j=1 and j=N. The conditions at the two boundaries can be represented as

$$\begin{aligned} C_1[\hat{S} - F_1(\kappa_1)] + C_2[\hat{S} - F_1(\kappa_2)] = 0 \\ C_1[\hat{S} - F_N(\kappa_1)] + C_2[\hat{S} - F_N(\kappa_2)] = 0 \end{aligned} \tag{26}$$

where F_1 and F_N are the functional relations resulting from substituting the eigenvector and eigenvalue into the expressions at grid-points j=1 and j=N, respectively. Note that $\hat{S} = \hat{S}(\kappa)$, and that every term is a function of κ. It is apparent that no general solution to this problem exists except the trivial one. Non-zero solutions exist for the condition where the determinant is equal to zero. The determinant condition gives the resulting expression for κ, the roots of which, with eqn (22), give the eigenvalues and eigenvectors of the system.

No closed form expressions are known for the roots to the determinant polynomial in this case or for any other reasonable boundary closures. The numerical solution of the determinant polynomial involves finding the roots of an "n^{th}" order polynomial in κ. It is apparent that the boundary conditions dramatically influence the eigenvalue spectrum in the matrix M. Only in the limit $N \rightarrow \infty$ do the boundary conditions decouple. The power of G-K-S theory comes from breaking the normal mode problem into three separate problems. The roots to the κ polynomials do not depend on the boundary to boundary coupling prevalent in eqns (25-26).

Theorem 2 describes what constitutes stability for the two IBVP's in Theorem 1 for the fully- or the semi-discrete case, and states that eqn(1) must satisfy the condition that no eigenvalues or generalized eigenvalues should exist for $\mathcal{R}(\mathrm{S}) \geq \eta_o$.

Both theorems 1 and 2 rely on a definition of an eigensolution for their quarter-plane analysis. Here, an eigensolution is presented for the semi-discrete case. Similar definitions exist for the fully discrete case. Referring to the semi-discretization defined by eqn (5),

Definition 4: An eigensolution for the IBVP defined by eqn (5) is the nontrivial function V(x,s) satisfying [8] :

I SV = M V $\quad x \geq 0$

II $V^I(0,s)$ - $TV^{II}(0,s) = 0$

III $\mathcal{R}(S) \geq 0$

IV for $\mathcal{R}(S) > 0$, V(x,s) is bounded as $x \rightarrow \infty$

V for $\mathcal{R} = 0$ and $|\kappa| = 1$, a perturbation inside the unit circle of κ ($|\kappa| = 1 - \epsilon, \epsilon > 0$) cannot produce an eigenvalue $\mathcal{R} > \delta, \delta > 0$.

Note that since $\psi = \psi_o \kappa^j$, condition (IV) implies $|\kappa| < 1$.

We refer to an eigensolution of the form (IV) or (V) as a G-K-S eigenvalue or a generalized G-K-S eigenvalue, respectively. With these conditions, the test for numerical stability has been simplified from the coupled normal mode analysis to tests involving $\mathcal{R}(S) > 0$, for $|\kappa| < 1$ at each boundary, plus the exceptional case when both $\mathcal{R}(S) = 0$, and $|\kappa| = 1$. Theorem 3 relates the stability of the semi-discretization to the stability of the fully discrete numerical method. Obviously, analogous stability definitions must be chosen for both the semi- and fully-discrete cases, specifically the generalized stability condition given by Definition 3. Theorem 3 relies on temporal advancement schemes which are locally stable numerical methods. For a locally stable numerical method, the stability domain $|z| \leq 1$ (z is the amplification factor) in the complex plane, encompasses within the LH-P an open semi-circle of radius "R_1" centered at the origin, and symmetric about the real axis. The standard fourth-order R-K method satisfies this condition. Discretizing time with the fourth-order R-K method in eqn (5) produces a fully discrete method defined by

$$V_j(t+k) = L(kM)V_j(t) + L(k)B_j g(t); \;\; j = 1, \ldots, N \tag{27}$$

where the time-step $\Delta t = k$, and where "L(kM)" is the polynomial in "k M" describing the time discretization. Then under very mild restrictions (see Kreiss [9]) on the eigenvalue structure of the matrix "L(kM)", if the semi-discrete approximation is stable in a generalized sense, the totally discrete approximation is stable in the same sense for $\|kM\| < R_1$.

We have outlined a systematic approach to addressing the finite domain stability problem for the fully-discrete numerical approximation to eqn (1). The remainder of this work will describe the application of these techniques to several higher-order finite difference schemes.

5. FOURTH-ORDER BOUNDARY CONDITIONS

Before proceeding with the stability analysis of various higher-order boundary conditions, an example is presented that illustrates the necessity of $(N-1)^{th}$ order boundary closure for an N^{th} order inner-scheme. The example also provides a numerical test to verify that the G-K-S theory is accurately predicting the stability behavior of the various numerical schemes. Consider the method-of-lines approximation to the scalar wave equation

$$\frac{\partial U}{\partial t} + \frac{\partial U}{\partial x} = 0, \ -1 \leq x \leq 1, \ t \geq 0 \tag{28}$$

$$U(t,-1) = \sin 2\pi(-1-t), \ U(0,x) = \sin 2\pi x \ \ -1 \leq x \leq 1, \ t \geq 0 \tag{29}$$

where the spatial discretization is accomplished by the fourth-order compact scheme described in detail by eqn (12). The exact solution is

$$U(t,x) = \sin 2\pi(x-t), \ -1 \leq x \leq 1, \ t \geq 0. \tag{30}$$

The comparison of the exact solutions with that obtained from various lower-order closures to the fourth-order inner-scheme provides a measure of the boundary influence. We begin by showing a grid convergence study performed to show the formal accuracy of the resulting schemes. The boundary condition formulas expressed at the grid-point "j=0" were

$$\frac{\partial V_0}{\partial x} + 2\frac{\partial V_1}{\partial x} = \frac{-5V_0 + 4V_1 + V_2}{2\Delta x} \tag{31}$$

$$\frac{\partial V_0}{\partial x} + \frac{\partial V_1}{\partial x} = \frac{-V_0 + V_1}{2\Delta x} \tag{32}$$

$$\frac{\partial V_0}{\partial x} = \frac{-V_0 + V_1}{\Delta x} \tag{33}$$

which represent third-, second-, and first-order closure at the inflow boundary, respectively. As mentioned earlier, the physical boundary condition was imposed at the point "j=0," and the actual closure occurs at the point "j=1". The closure could have been written explicitly for the point "j=1" by combining these formulas with the inner-scheme at "j=1"

$$\frac{\partial V_0}{\partial x} + 4\frac{\partial V_1}{\partial x} + \frac{\partial V_2}{\partial x} = \frac{-3V_0 + 3V_2}{\Delta x} \tag{34}$$

resulting in formula of the form

$$2\frac{\partial V_1}{\partial x} + \frac{\partial V_2}{\partial x} = \frac{-V_0 - 4V_1 + 5V_2}{2\Delta x} \tag{35}$$

$$3\frac{\partial V_1}{\partial x} + \frac{\partial V_2}{\partial x} = \frac{-V_0 - 2V_1 + 3V_2}{\Delta x} \tag{36}$$

$$4\frac{\partial V_1}{\partial x} + \frac{\partial V_2}{\partial x} = \frac{-2V_0 - V_1 + 3V_2}{\Delta x}. \tag{37}$$

At the outflow boundary, closure was accomplished with the expressions

$$\frac{\partial V_N}{\partial x} + 2\frac{\partial V_{N-1}}{\partial x} = -\frac{-5V_N + 4V_{N-1} + V_{N-2}}{2\Delta x} \tag{38}$$

$$\frac{\partial V_N}{\partial x} + \frac{\partial V_{N-1}}{\partial x} = -\frac{-V_N + V_{N-1}}{2\Delta x} \tag{39}$$

$$\frac{\partial V_N}{\partial x} = -\frac{-V_N + V_{N-1}}{\Delta x} \tag{40}$$

which represent third-, second-, and first-order spatial accuracy, respectively. These expressions are valid for the point "j=N" since there is no physical condition to impose there.

In all cases, the temporal discretization was accomplished with the fourth-order Runge-Kutta algorithm. At every iteration, the solution was advanced for the grid-points "j=0,N", followed by the imposition of the boundary condition at the point "j=0." Since the inflow boundary condition was a nonlinear function of time, care was taken to evaluate the function corresponding to the proper intermediate level in time. Failure to do so degraded the formal accuracy of the method. The CFL used in the simulations was in the range $0.1 \leq CFL \leq 1$. In no case did this violate the Von Neumann stability condition for the Cauchy problem. It should be noted that the formal truncation of the method is $O(\Delta t^4)$, and the error in time decays to the fourth power of the CFL for a given grid, and can be made as small as desired by decreasing the CFL. Typically, CFL's ≤ 0.1 were not needed since the dominant terms in the modified equation were negligible compared with spatial terms. Further reduction of the CFL resulted in no change in the error of the scheme. Recognition of this fact allows one to test the formal accuracy of methods with spatial accuracy higher than fourth-order for sufficiently small values of the CFL, and was used in the sixth-order simulations to determine formal accuracy. Finally, a third-order Runge-Kutta was used to test the generality of the temporal discretization in several cases. The results were quantitatively similar.

The simulations were all run to equivalent times T=25, for all grids and methods at a CFL of 0.25. The error at T was then calculated and reported as an L_2 norm. The L_∞ norm produced similar results, but is not reported here. For methods which are Lax-stable, the error is bounded uniformly at each stage for $0 < \Delta t < \tau$ and $0 \leq k\Delta t \leq T$, where k is the number of time-steps. Doubling the grid at constant CFL, should decrease the error at time

level T by a factor $\frac{1}{2}^p$ where "p" is the order of the method. The formal accuracy of each scheme was determined for each of the Lax-stable schemes in this manner.

Figures 1-3 show the results of this study. The $\log_{10}$ of the L_2 error is plotted as a function of the $\log_{10}$ of the number of grid-points resolving one period of the sine wave. The grid density ranges from 10 to 25 grid-points/(2π radians). Note that once a threshold accuracy is attained the points appear to decrease linearly. The slope of the data (dY/dX) gives the apparent formal accuracy of the method. In all cases, formal fourth-order accuracy is obtained with third- or fourth-order boundary conditions. Second order closure results in third-order formal accuracy, and first-order closure results in second-order accuracy. It is also apparent that the accuracy is greater for the fourth-order than for the third-order closure, regardless of the formal accuracy. These results are in agreement with the theory of Gustafsson [3] predicting that to retain formal accuracy of a numerical method, boundary conditions of order (N-1) must be imposed to retain N^{th} order. Another interesting feature is that imposition of lower-order boundary conditions at the outflow plane results in a greater degree of error than at the inflow plane. One might have thought that since the characteristic is pointing out of the domain at the outflow boundary, error would be swept immediately out of the domain. This is obviously not the case.

We will now derive the formal stability of the numerical boundary conditions used in this example. It can be shown that the fourth-order compact scheme is "Cauchy stable" for CFL ≤ 1.63. The stability of the inflow and outflow boundary conditions on the semi-infinite domain must be demonstrated. We begin by testing the outflow stability. The partial differential equation is

$$\frac{\partial U}{\partial t} - \frac{\partial U}{\partial x} = 0, \;\; x \geq 0, \;\; t \geq 0. \tag{41}$$

No boundary condition is required in this problem, although a NBS is imposed at x = 0. As was done on the normal mode analysis for the finite domain, we assume a solution of the form $V_j(t) = \exp^{St} \phi_j$, where $\phi_j = \phi_o \kappa^j$. Substitution into the inner scheme produces the resolvent condition for the eigenvalue $\hat{S}$

$$(\frac{1}{\kappa} + 4 + \kappa)\hat{S} = 3(\frac{-1}{\kappa} + \kappa) \tag{42}$$

at each grid-point $j \geq 1$. At grid-point j=0, the scheme was closed with one of the boundary expressions given in eqns (12, 38, 39, 40) (obviously written for the grid-point j=0). Substitution of $V_j(t)$ into these expressions yields

$$(6 + 18\kappa)\hat{S} = -17 + 9\kappa + 9\kappa^2 - \kappa^3 \tag{43}$$

$$(2 + 4\kappa)\hat{S} = -5 + 4\kappa + \kappa^2 \tag{44}$$

$$(1+\kappa)\hat{S} = -2+2\kappa \tag{45}$$

$$\hat{S} = -1+\kappa. \tag{46}$$

Solving eqn (42) for $\hat{S}$ and substituting into eqns (43, 44, 45, 46) yield polynomials in κ of the form

$$\frac{(\kappa-1)^5}{(\kappa^2+4\kappa+1)} = 0 \quad (4^{th}) \tag{47}$$

$$\frac{(\kappa-1)^4}{(\kappa^2+4\kappa+1)} = 0 \quad (3^{rd}) \tag{48}$$

$$\frac{(\kappa-1)^3}{(\kappa^2+4\kappa+1)} = 0 \quad (2^{nd}) \tag{49}$$

$$\frac{(\kappa-1)^2(\kappa+2)}{(\kappa^2+4\kappa+1)} = 0 \quad (1^{st}). \tag{50}$$

Clearly, the only value of κ which will simultaneously satisfy the inner resolvent condition and any of the outflow boundary conditions is $\kappa = 1$. Substitutions of $\kappa = 1$ into the resolvent condition produces $\hat{S} = 0$, the case for which the perturbation test in G-K-S theory (condition V) must be used to show stability. Substituting $\kappa = 1-\epsilon$ into the resolvent condition produces to first order

$$6\hat{S} = -6\epsilon. \tag{51}$$

For $\epsilon > 0$ and $|\kappa| < 1$, $\hat{S} < 0$ showing stability of the perturbation. All the tested outflow boundary conditions are G-K-S stable. Thus, $\kappa = 1$ is not a generalized eigenvalue.

To show stability of the inflow conditions we study the partial differential equation

$$\frac{\partial U}{\partial t} + \frac{\partial U}{\partial x} = 0, \;\; x \geq 0, \;\; t \geq 0; \tag{52}$$

with the boundary condition imposed at x = 0 of the form

$$U(0,t) = g(t), \quad t \geq 0. \tag{53}$$

In spite of the physical boundary condition being imposed at j=0, a NBS must be imposed at j=1, and must be tested for stability. Substituting $V_j(t) = \exp^{St}\phi_j$, where $\phi_j = \phi_o\kappa^j$, into the inner-scheme produces the resolvent condition identical to eqn (42). Substitution into the first through fourth-order boundary conditions defined by eqns (12, 35, 36, 37), produce equations for $\hat{S}$ of the form

$$(6+6\kappa)\hat{S} = -9+9\kappa+\kappa^2 \tag{54}$$

$$(4+2\kappa)\hat{S} = -4+5\kappa \tag{55}$$

$$(6+\kappa)\hat{S} = -4+6\kappa \tag{56}$$

$$(4+2\kappa)\hat{S} = -2+6\kappa. \tag{57}$$

Note that without loss of generality, we have assumed g(t) = 0 on the inflow boundary j=0. This eliminates the influence of j=0 in the boundary polynomial, and reduces the order of the polynomials by one. Solving the resolvent equation for $\hat{S}$ and substituting into eqns (54, 55, 56, 57) yields polynomials in κ of the form

$$\frac{(\kappa^4 - 5\kappa^3 + 10\kappa^2 - 9\kappa + 9)}{(\kappa^2 + 4\kappa + 1)} = 0 \quad (4^{th}) \tag{58}$$

$$\frac{(\kappa^3 - 4\kappa^2 + 5\kappa - 8)}{(\kappa^2 + 4\kappa + 1)} = 0 \quad (3^{rd}) \tag{59}$$

$$\frac{(\kappa^2 - 2\kappa + 7)}{(\kappa^2 + 4\kappa + 1)} = 0 \quad (2^{nd}) \tag{60}$$

$$\frac{(\kappa^2 - 2\kappa - 11)}{(\kappa^2 + 4\kappa + 1)} = 0 \quad (1^{st}) \tag{61}$$

$$\tag{62}$$

the roots of which are

$$\kappa = 2.286 \pm 1.215i, \mathit{0.2134 \pm 1.138i} \quad (4^{th}) \tag{63}$$

$$\kappa = 3.218, 0.3906 \pm 1.527i \quad (3^{rd}) \tag{64}$$

$$\kappa = 1 \pm \sqrt{6}i \quad (2^{nd}) \tag{65}$$

$$\kappa = 1 \pm 2\sqrt{3}i \quad (1^{st}) \tag{66}$$

where $i = \sqrt{-1}$. It is apparent that $|\kappa| > 1$ in all of these expressions. There are no eigenvalues or generalized eigenvalues, and the inflow boundary is stable to these closures. Given that the Cauchy problem and the two quarter-plane problems are stable, implies that the finite domain problem defined in eqn (12) is G-K-S stable for all boundary conditions specified thus far.

A more rigorous example of the ability of the G-K-S theory to predict the stability of the fourth-order compact scheme is demonstrated by a pathological inflow boundary scheme. Since the inflow problem involves a NBS at the grid-point j=1 which is biased in the "down-wind" direction, we suspect that it will be more sensitive to instability than the outflow boundary. We formulate a boundary scheme, which is a linear combination of the first- and second-order schemes, noting that they both have been shown to be stable boundary treatments. The resulting scheme which we shall use at the inflow boundary is

$$(1 + 2\beta)\frac{\partial V_0}{\partial x} + \frac{\partial V_1}{\partial x} = 2(1 + \beta)\frac{-V_0 + V_1}{\Delta x} \tag{67}$$

where β is the amount of first-order influence in the formula. For $\beta = 0$, the standard second-order closure is obtained. For all other values of β, the scheme is formally first-order accurate.

We shall denote this scheme as (1^1-4-4) since the inflow boundary is a one-parameter family of first order schemes, and the outflow is closed with a fourth-order formula. As was done previously, the dependence of the formula on the space derivative at j=0 is eliminated from eqn (67) by the inner-scheme written at j=1. The resulting expression is

$$[2(1+2\beta)-\frac{1}{2}]\frac{\partial V_1}{\partial x}+\frac{(1+2\beta)}{2}\frac{\partial V_2}{\partial x} \;=\; \frac{-(1+4\beta)V_0-2(1+\beta)V_1+3(1+2\beta)V_2}{2\Delta x}. \quad (68)$$

Substituting $V_j(t)=\exp^{St}\phi_j$, $\phi_j=\phi_o\kappa^j$ into eqn (68) and noting the expression must be valid for the case g(t) = 0, results in a boundary scheme of the form

$$([2(1+2\beta)-\frac{1}{2}]+\frac{(1+2\beta)}{2}\kappa)\hat{S}=-(1+\beta)+\frac{3}{2}(1+2\beta)\kappa. \quad (69)$$

Solving for $\hat{S}$ from the inner scheme eqn (42) and substituting it into eqn (69) produces a polynomial in κ of the form

$$(-1+2\beta)\kappa^2+(2-4\beta)\kappa-(7+22\beta)=0. \quad (70)$$

Solving for κ yields

$$\kappa=1\pm\sqrt{6}\sqrt{\frac{(4\beta+1)}{(2\beta-1)}},\;\; \beta\neq\frac{1}{2}. \quad (71)$$

A double root exists for $\beta=\frac{-1}{4}$ and $\kappa=1$. Substituting $\kappa=1$ into the resolvent expression yields $\hat{S}=0$, and a perturbation test shows that the boundary exhibits a generalized eigenvalue instability. Further inspection of eqn (71) shows that $|\kappa|\leq 1$ over the range $\frac{-5}{8}\leq\beta\leq\frac{-1}{4}$. All other values of β need not be considered as candidates for instability since $|\kappa|>1$. Substitution of the expression for κ obtained from eqn (71), into eqn (69), yields an expression for $\hat{S}$ in terms of the parameter β. Numerical evaluation of this expression shows that $\mathcal{R}(\hat{S})\geq 0$ for $-.37\leq\beta\leq\frac{-1}{4}$. Thus, an eigensolution exists for this range, and the coupled inner-boundary scheme is unstable.

To verify these findings, the model scalar wave equation described by eqns (28, 29, 30), was solved with the pathological inflow boundary conditions describe in eqn (67). Fourth-order boundary conditions were used at the outflow boundary. Figure (4) shows the results of the numerical investigation. Plotted is the $\log_{10}$ of the L_2 error of the solution integrated to a fixed time "T," as a function of the parameter β, ranging from $[\frac{-1}{2},\frac{1}{2}]$. Two grid densities are shown in the study, and behave similarly. The theoretically predicted range of instability $-.37\leq\beta\leq\frac{-1}{4}$ is replicated in the numerical study to within graphical limitations of the plot. In the unstable regime, the error grew exponentially with the number of iterations required to reach the time level T, and quickly became very large.

Although these boundary conditions are pathological, this study points to the fact that imposition of a first-order inflow boundary conditions is not sufficient to guarantee stability with the fourth-order compact inner-scheme. A similar experiment was performed on the outflow boundary using a linear combination of first- and second-order boundary conditions. For those boundary conditions, no eigensolutions could be found. That is not to imply that a completely arbitrary outflow boundary condition of at least first-order accuracy is always stable. It does indicate that the outflow is less susceptible to instabilities than the inflow boundary.

Another note is appropriate, concerning the complexity of the G-K-S analysis for compact schemes. For the fourth-order compact inner-scheme, the polynomial of the highest degree which could not be factored (resulting in a numerical solution) was of degree four, and resulted from the closure with the fourth-order boundary conditions at the inflow plane. The G-K-S analysis of the fourth-order explicit scheme described by eqn (9) was performed by Strikwerda [8]. Stability polynomials of order eight were obtained for fourth-order closure at the inflow plane. It is apparent that the stability polynomials resulting from compact stencils are simpler expressions. This simplicity (and MACSYMA) will allow us to analyze schemes of sixth-order spatial accuracy without insurmountable algebraic polynomials at each boundary.

6. SEMI-DISCRETE EIGENVALUE ANALYSIS

The uniformly fourth-order explicit scheme (4,4-4-4,4) analyzed by Strikwerda [8] and the uniformly fourth-order compact scheme (4-4-4) presented here are both G-K-S stable for the semi-discrete problem and, therefore, will exhibit generalized stability for the fully discrete problem if advanced with a locally stable temporal scheme. This definition of stability ensures that the error of the numerical solution will remain uniformly bounded for all times by an exponentially growing amount. The exponential growth rate of the error is asymptotically (N $\rightarrow \infty$, where N is the total number of grid-points used) independent of the grid used. Thus, grid refinement studies with these methods, performed by integrating the governing equation to a fixed time level T on successively finer grids will demonstrate that the numerical solution converges to the exact solution at a rate of at least the order of the method.

A disturbing feature of this stability definition is that the solution is not required to remain bounded for all times, even though the physical solution remains bounded for all times. Figure (5) shows a grid refinement study performed with the fourth-order compact (4-4-4) scheme demonstrating this behavior. The model equation was that described by eqns (28, 29, 30); the time interval was $0 \leq t \leq 100$ and the grids used were 21, 41, and 81 grid-points, respectively. Time was advanced with a fourth-order Runge-Kutta scheme in all

cases. The exact solution is a traveling sine wave of amplitude 1, for all times. Shown is the log_{10} of the L_2 error, plotted as a function of time. Simulations on all three grids were run at various CFL's. The initial portion of the simulation is characterized by nearly constant levels of error on all three grids. After a sufficiently long time, the unstable modes in the numerical solution dominate the spatial truncation error. From that point on, the solution diverges exponentially from the exact solution. Note that the growth rate in time, of the unstable modes of the solution is nearly grid independent, and that at any time T refining the grid by a factor of two results in a factor of 16 decrease in the error. It is also evident that at large times the actual error will be exponentially large. An interesting feature of the numerical method is that the exponential growth of the solution is dependent on the CFL used to advance the solution. For CFL = 1, the solution does not grow in time, while for CFL $\leq \alpha$ (α is some critical value less than CFL_{max}), exponential growth is observed. (This feature will be explained later, in terms of the amplification factor of the scheme.) Regardless of the CFL, fourth-order convergence is observed with the scheme.

To understand the fundamental nature of the fixed grid, temporal divergence of the solution in the previous example, it is instructive to study the eigenvalue spectrum of the spatial discretization operator. As a semi-discretization, eqn (28) can be written in the form of eqn (5) as

$$\frac{dV_j}{dt} = MV_j + B_j g(t), \;\; j = 1, \; ..., N \tag{72}$$

where M is the N x N matrix describing the spatial discretization operator, and B_j g(t) represents the physical boundary data. Assuming that

$$P^{-1}MP = S; \;\; P^{-1}U = V; \;\; P^{-1}Bg(t) = H \tag{73}$$

where S is a diagonal matrix, and P^{-1} and P are similarity transforms composed of the left and right eigenvectors of the matrix M, respectively, eqn (72) takes the form

$$\frac{dU_j}{dt} = SU_j + H_j, \;\; j = 1, \; ..., N. \tag{74}$$

The solution to eqn (74) is

$$U_j(t) = \exp^{S_j t} U_j(0) + \int_0^t \exp^{S_j(t-\tau)} H_j(\tau) d\tau, \;\; j = 1, \; ..., N. \tag{75}$$

In this form, the solution to eqn (74) depends exponentially on the eigenvalues S_j of the matrix M. Note that this solution assumes that the eigenvalues S_j are not degenerate, and that H(t) is not at a resonance frequency. If either of these situations occur, then the solution would include terms proportional to $t^p \exp^{S_j t}$, where "p" is the order of the degeneracy. The

precise behavior depends on the temporal nature of H(t), but in general, for boundary data which remains bounded for all time, the solution grows only for the modes which have eigenvalues S_j with positive real parts. In addition, the growth rate will be governed by the eigenvalue with the largest positive component. Thus, any spatial discretization to the semi-discrete problem defined in eqn (72) will exhibit exponential divergence of the solution from the bounded physical solution, if it has an eigenvalue in the right half of the complex plane.

Figures (6-7) show the eigenvalue spectrum resulting from the explicit fourth-order and the compact fourth-order spatial operators, closed at the boundaries with schemes of third- or fourth-order accuracy. In shorthand nomenclature, the explicit cases (3,3-4-3,3) and (4,4-4-4,4) are shown in Figure (6), and the compact cases (3-4-3) and (4-4-4) are shown in Figure (7). The spectrums are shown on grids of 21, 41, and 81 points, respectively. Note that closing the inner-schemes with third order NBS in both cases results in an eigenvalue spectrum which is bounded to the Left Half-Plane (LH-P), and that the uniformly fourth-order schemes cross over the imaginary axis into the Right Half-Plane (RH-P) of the complex plane.

For long times, the maximum eigenvalues from the uniformly fourth-order schemes very accurately predict the exponential growth of the solution. In Figure (5), the solutions obtained from the (4-4-4) compact scheme grow exponentially in time. Assuming the error can be represented functionally as $\epsilon_N(t) = \epsilon_N(0)\exp^{\alpha_N t}$, where N is the number of grid-points used in the spatial discretization, a growth rate α_N can be determined numerically. Similarly, from an eigenvalue determination, an effective grow rate α_S defined by $\exp^{\alpha_S N\Delta t} = |G_{max}(\Delta t)|^N$, can be calculated, where G_{max} is the numerical amplification obtained from the temporal advancement scheme. For the fourth-order Runge-Kutta scheme

$$G_j = 1 + S_j\Delta t + \frac{(S_j\Delta t^2)}{2!} + \frac{(S_j\Delta t^3)}{3!} + \frac{(S_j\Delta t^4)}{4!}, \quad j = 1, \ldots, N \tag{76}$$

and $|G_{max}|$ will frequently correspond to the maximum eigenvalue $\mathcal{R}(S_{max})$. Table (1) shows a comparison of the observed growth rate of the (4-4-4) compact scheme with that predicted from an eigenvalue determination. In each case, the maximum eigenvalue is used to predict the temporal grow of the solution.

Grid	$\alpha_{Numerical}$	$\alpha_{\mathcal{R}(S_{max})}$
21	0.1321	0.1315
41	0.1476	0.1474
81	0.1537	0.1479

Table 1: Numerical vs. Theoretical Growth Rate; (4-4-4).

The agreement is very good, with a slight discrepancy in the comparison on the 81 grid-point case. In Figure (5), note the oscillatory nature of the growth of the solution. The uncertainty of the phase of the solution accounts for the discrepancy in the predicted growth rate in that case.

A necessary condition for Lax stability of the finite domain semi-discretization can be expressed in terms of the eigenvalues of the spatial matrix operator as

$$\mathcal{R}(S_j) \leq \omega; \;\; \omega \geq 0; \;\; j = 1, \ldots, N \tag{77}$$

where S_j are the eigenvalues of the spatial operator, and N is an arbitrary number. It is apparent that the eigenvalue structure asymptotically approaches a bound in the RH-P as $N \rightarrow \infty$. All the fourth-order schemes presented thus far have satisfied this constraint. For the third-order NBS's (3,3-4-3,3) and (3-4-3), the constant is $\alpha = 0$, while for the fourth-order NBS's, the constant is greater than zero.

As mentioned earlier, a curious feature of the (4-4-4) (as well as other high-order spatial schemes) is that the growth of the solution is CFL dependent on all grids. For CFL's close to the CFL_{max}, as determined from Von Neumann stability analysis, the schemes are bounded in time. For sufficiently small CFL's, the schemes begin to diverge exponentially in time. (Again, it should be emphasized that in either case, the scheme is still G-K-S or Lax stable.) This behavior can be explained by noting a particular feature of the fourth-order Runge-Kutta time advancement scheme as well as some of the other locally stable time schemes. The stability bound of a time advancement scheme is defined as the locus of points in the complex plane where $|z| \leq 1$. Clearly, $|z| = 1$ divides the plane into two regions. When the spatial eigenvalues (scaled by Δt) of a particular discretization lie entirely within the $|Z| = 1$ boundary, the combined time-space scheme is generally stable. The stability regime of these schemes includes a semi-circular portion of the complex plane, centered at the origin and symmetric about the real axis and extending into the left half-plane. In addition, they contain a small part of the right half-plane, although not near the origin. If the spatial eigenvalues which lie in the RH-P are encompassed by the $|Z| = 1$ boundary, the resulting scheme is stable. If a Δt is chosen such that the $|Z| = 1$ line does not contain the RH-P eigenvalues, then the solution diverges with time. Figure (8) shows this feature for the (4-4-4) spatial scheme and the fourth-order Runge-Kutta scheme in time. For CFL's which are near the CFL_{max}, the maximum amplification rate $|G_{max}|$ is less than one. For sufficiently small CFL's, the $|G_{max}| > 1$ by an amount that is proportional to $\mathcal{R}(S_{max})$, and the solution will diverge exponentially in time. It can be shown that a spatial scheme that has RH-P eigenvalues can always be made to diverge exponentially for sufficiently small CFL's if a conventional third- or fourth-order R-K time advancement scheme is used.

7. ASYMPTOTIC STABILITY

The previous discussion of Figure (5-8) brings out a subtle point in the Lax stability theory. In dealing with the numerical integration of time-dependent partial differential equations, there are different limit processes that can be considered. One limit is the behavior of the numerical solution as the mesh size $\Delta x \to 0$ for a fixed time T. Another is the behavior of the solution for a fixed mesh as the time T tends to infinity.

Stability, in the sense of Lax, addresses the first issue: boundedness of the numerical solutions as the mesh is refined at a fixed *physical time*. The essence of the Lax equivalence theorem is that if the numerical solution is bounded in this sense, then it converges to the true solution in the limit $\Delta x \to 0$. To obtain an approximation to the true solution at time T, one integrates the IBVP up to time T on a sequence of grids as $\Delta x \to 0$. This sequence converges to the exact solution for all time levels T.

Nothing in this definition excludes growth in *time*, and specifically allows exponential growth in time (see eqn (18)). Moreover, even if each of the quarter-plane problems is stable and allow no growth in time, the combined finite interval problem still allows exponential growth in *time*. (The Laplace transforms used in the G-K-S theory are legitimate only if growth in time is allowed.)

Unfortunately, for genuinely time dependent problems, this stability definition might be too weak, in particular if long time integration is being carried out. The reason is that in order to achieve any reasonable accuracy for large times, one needs an excessive number of grid points. For long time numerical simulations to be useful, the solution of the semi-discrete problem defined in eqn (5), must be bounded in time as well. This means that for a fixed mesh N, the eigenvalues of the matrix M in eqn (5) have non-positive real part, and those with zero real part have (geometrical) multiplicity of 1. This is called **Asymptotic Stability**.

An irksome feature of asymptotic stability is that, by itself, asymptotic stability does not imply Lax stability. There are numerous examples in the literature of fully discrete schemes that are asymptotically stable, but not Lax stable. The classic example of this is the case of a first order upwind spatial operator being advanced with an Euler explicit time advancement scheme. The eigenvalues for the fully discrete system are $(1 - \lambda)$, occurring a degenerate N times. Eigenvalue determination suggests that the CFL of the scheme should be 2, whereas, Von Neumann analysis and practical experience suggests that a CFL of one is the maximum stable CFL. The discrepancy can be explained by the fact that for $1 < CFL < 2$, the matrix norm first grows rapidly before decaying asymptotically to zero. One might have suspected this difficulty by noting that in the semi-discrete case, the degenerate eigenvalues give rise to geometric growth in time, only later to be dominated by the exponentially decaying terms in the expressions.

An example for the semi-discrete case is now presented. Consider eqn (5) with $g(t) = 0$. Let the matrix M be defined by the second-order central difference operator for the interior points. In matrix form, M can be written as

$$M = \frac{1}{2}\begin{bmatrix} -1 & 1 & & & & & \\ -1 & 0 & 1 & & & 0 & \\ & \cdot & \cdot & \cdot & & & \\ & & \cdot & \cdot & \cdot & & \\ & & & \cdot & \cdot & \cdot & \\ & 0 & & & -1 & 0 & 1 \\ & & & & & -1 & 1 \end{bmatrix} \tag{78}$$

where the boundary closures at grid-points j=1 and j=N are artificially chosen. Using semi-discrete modal analysis, we determine a solution to eqn (5) by assuming the form $V_j(t) = \exp^{St}\phi_j$, with $\phi = A\kappa^j + B(\frac{-1}{\kappa})^j$. The resolvent condition from the interior scheme yields $S_j = \frac{1}{2}(\kappa - \frac{1}{\kappa})$. Using the boundary conditions at point j=1 and j=N to determine the values of A and B yields the expression for κ of the form

$$(\kappa + 1)((-1)^N - \kappa^{2N}) = 0. \tag{79}$$

The roots to eqn (79) are $\kappa = -1$ and $\kappa = i\exp^{\frac{i\pi j}{N}}$ for j=1,N-1. The eigenvalues are thus: S = 0 and S = $i\cos\frac{\pi j}{N}$ for j=1,N-1, and are purely imaginary. The spatial discretization satisfies our definition of asymptotic stability for values of N, which are odd.

The spatial discretization defined by eqn (78) admits a generalized eigenvalue instability at the inflow boundary. Using G-K-S analysis for the inflow boundary produces compatibility equations of the form

$$\begin{aligned} 2\hat{S}\,\kappa &= \kappa - 1, \;\; j = 1 \\ 2\hat{S}\,\kappa^2 &= \kappa^3 - \kappa, \;\; j = 2 \end{aligned} \tag{80}$$

for which the only solution is $\kappa = 1$, $\hat{S} = 0$. The boundary condition is unstable to perturbations away from the unit circle and, therefore, exhibits a generalized eigenvalue instability at the boundary. It is apparent that asymptotic stability for the semi-discrete problem does not guarantee Lax stability.

In addition to the previously mentioned examples, Reddy and Trefethen [14] have shown that it is not sufficient to consider the exact eigenvalues in determining the stability of a method. The famous Kreiss matrix theorem gives necessary and sufficient conditions for Lax stability in terms of the eigenvalues of the matrix M. A useful and equivalent test for determining stability is the analysis of the resolvent condition, which Reddy and Trefethen interpreted as involving not only the eigenvalues of the matrix M but also the ϵ-pseudo-spectrum of the discretization matrix. This pseudo-spectrum is obtained by perturbing

the matrix M by an arbitrary matrix of norm ϵ. Examples where the ϵ-pseudo-eigenvalues determine the stability bounds of numerical methods are given by Reddy et al. [14]. It is apparent that basing a stability definition on the eigenvalue determination of the spatial operator is not sufficient for stability. It is, however, useful for the present applications of higher-order scheme to restrict the allowable numerical discretizations to those possessing Lax stability and the property of bounded LH-P eigenvalues. For a broad class of spatial discretizations, these constraints are sufficient for the stability of the resulting numerical scheme. It is concluded that constraining the spatial operators to those possessing these properties is a useful and fairly general enhancement, and will be pursued in the remainder of this work.

Before leaving fourth-order spatial discretizations, it is desirable to devise a uniformly fourth-order scheme. We already know that conventional discretization formulas at the boundaries result in G-K-S stable, but not asymptotically stable schemes for both the explicit and compact cases. The NBS's used in each case relied on optimal order schemes at the boundary, where N+1 constraints were used to devise the N^{th} order scheme. Specifically, five grid-points in the explicit case, and four grid-points and one derivative condition in the compact case. If one removes the constraint of using optimal schemes at the boundaries, NBS with different dissipative characteristics can be devised and an asymptotically stable spatial scheme which is uniformly fourth-order can be found.

We begin by devising an asymptotically stable fourth-order compact scheme, which we shall denote as (4^3-4-4^3). The "4^3" signifies that the boundary point is closed with a fourth-order three-parameter family of schemes. The scheme defined at grid-point j=0 can be written as

$$\frac{\partial U_0}{\partial x} = (C_0U_0 + C_1U_1 + C_2U_2 + C_3U_3 + C_4U_4 + C_5U_5 + C_6U_6 + C_7U_7)/(\Delta x). \tag{81}$$

To be formally fourth-order accurate, Taylor series truncation analysis relates the coefficients in the following manner

$$\begin{aligned}
C_0 &= -(\alpha - 28\beta + 322\gamma + 13068)/5040 \\
C_1 &= +(\alpha - 27\beta + 295\gamma + 5040)/720 \\
C_2 &= -(\alpha - 26\beta + 270\gamma + 2520)/240 \\
C_3 &= +(\alpha - 25\beta + 247\gamma + 1680)/144 \\
C_4 &= -(\alpha - 24\beta + 226\gamma + 1260)/144 \\
C_5 &= +(\alpha - 23\beta + 207\gamma + 1008)/240 \\
C_6 &= -(\alpha - 22\beta + 190\gamma + 840)/720 \\
C_7 &= +(\alpha - 21\beta + 175\gamma + 720)/5040
\end{aligned} \tag{82}$$

with similar expressions defined for the closure at the other end of the domain. By systematically searching the three-parameter space spanned by the parameters α, β, and γ, coefficients can be obtained which yield an eigenvalue spectrum which is bounded to the LH-P. The values of α, β, and γ are not unique, and no attempt to optimize the spectrum was made. A particular set of coefficients which make the scheme asymptotically stable are $\alpha = -1560, \beta = -355$ and $\gamma = -35$. Figure (9) shows the resulting spectrum from the (2-4-2), (3-4-3) and (4^3-4-4^3) schemes. In all cases the eigenvalues are bounded to the LH-P, and the resulting scheme is asymptotically stable.

Since the asymptotic stability condition $\mathcal{R}(S_j) \leq \omega$ for $\omega = 0$ is a very strong necessary condition, but not a sufficient condition, we still must show G-K-S stability for this case. For the outflow problem the model equation is

$$\frac{\partial U}{\partial t} - \frac{\partial U}{\partial x} = 0, \;\; x \geq 0, \;\; t \geq 0; \tag{83}$$

no boundary condition is required in this problem, although a NBS is imposed at x = 0. Assuming a solution of the form $V_j(t) = \exp^{St} \phi_j$, where $\phi_j = \phi_o \kappa^j$, and substitution into the inner scheme produces the resolvent condition for the eigenvalue $\hat{S}$

$$(\frac{1}{\kappa} + 4 + \kappa)\hat{S} = 3(\frac{-1}{\kappa} + \kappa) \tag{84}$$

at each grid-point $j \geq 1$. At grid-point j=0, the parameter scheme produces an equation of the form

$$360\hat{S} \;\; = \;\; -(+727 - 1370\kappa + 1110\kappa^2 - 875\kappa^3 + 775\kappa^4 - 552\kappa^5 + 220\kappa^6 - 35\kappa^7). \tag{85}$$

Solving the resolvent condition for $\hat{S}$ and substituting into the boundary scheme yields a polynomial in κ of the form

$$(\kappa - 1)^5(35\kappa^4 + 95\kappa^3 - 168\kappa^2 - 227\kappa - 353) = 0. \tag{86}$$

Solving the polynomial for κ produces no roots which are in magnitude less than one: thus, a stable condition. The possibility of $\kappa = 1$ exists and must be checked for generalized eigenvalues. The condition is the same one tested for outflow stability in eqn (51), and was shown to be stable. Thus, the parametric fourth-order outflow scheme is G-K-S stable for the parameters α, β and γ presented above.

To show stability of the parameter scheme at the inflow, we study the partial differential equation

$$\frac{\partial U}{\partial t} + \frac{\partial U}{\partial x} = 0, \;\; x \geq 0, \;\; t \geq 0; \tag{87}$$

with the boundary condition imposed at x = 0 of the form

$$U(0,t) = g(t), \quad t \geq 0. \tag{88}$$

Eliminating $\frac{\partial U_0}{\partial x}$ between the boundary scheme at j=0 and the inner-scheme at j=1, yields a combination boundary scheme of the form

$$\begin{aligned} 1440\frac{\partial U_1}{\partial x} + 360\frac{\partial U_2}{\partial x} &= -(+353U_0 + 1370U_1 - 2190U_2 + 875U_3 - 775U_4 \\ &\quad +552U_5 - 220U_6 + 35U_7)/(\Delta x) \end{aligned} \tag{89}$$

Substituting $V_j(t) = \exp^{St}\phi_o\kappa^j$ into the inner-scheme and the boundary scheme produces the resolvent condition eqn (42), and

$$\begin{aligned} (1440\kappa + 360\kappa^2)\hat{S} &= (+353U_0 + 1370\kappa^1 - 2190\kappa^2 + 875\kappa^3 - 775\kappa^4 + 552\kappa^5 \\ &\quad -220\kappa^6 + 35\kappa^7). \end{aligned} \tag{90}$$

Solving eqn (42) for $\hat{S}$ and substituting into eqn (91), with the condition that $U_0 = 0$ yields a polynomial in κ of the form

$$\kappa(-2950 + 2210\kappa^1 - 2195\kappa^2 + 1615\kappa^3 - 1673\kappa^4 + 1213\kappa^5 - 293\kappa^6 - 80\kappa^7 + 35\kappa^8) = 0. \tag{91}$$

Solving this polynomial results in no roots for which $|\kappa| < 1$. The only possibility for instability is the condition $|\kappa| = 1$. Again, this condition was checked previously for the other fourth-order schemes, and was shown to be stable for the inflow. The compact three-parameter family (4^3-4-4^3) is stable for inflow and outflow, if the parameters are $\alpha = -1560, \beta = -355$ and $\gamma = -35$. In addition, the scheme produces an eigenvalue spectrum for the scalar wave equation which is bounded to the Left Half-Plane. It can be shown that treating the inflow and outflow boundaries of the explicit fourth-order scheme in a similar manner (4^3,4-4-4,4^3) also produces an asymptotically stable scheme. Whether the resulting scheme is G-K-S stable was not checked in this work.

8. SIXTH-ORDER SCHEMES

As a last step in this work, the ideas and techniques used to analyze the fourth-order compact schemes are applied to sixth-order compact schemes. All the schemes tested here will be based on the sixth-order compact inner-scheme developed by Lele [15]. The scheme can be written in the form

$$\frac{\partial U_{j-1}}{\partial x} + 3\frac{\partial U_j}{\partial x} + \frac{\partial U_{j+1}}{\partial x} = \frac{-U_{j-2} - 28U_{j-1} + 28U_{j+1} + U_{j+2}}{12\Delta x}; \; j = 2, \ldots, N-2. \tag{92}$$

The scheme utilizes information from five-point explicitly and three point implicitly. As a consequence of the five point width of the stencil, NBS's must be provided at two points at each end of the domain (j=0,1 and j=N-1,N). The physical boundary condition is used at one of the inflow points. To ensure formal sixth-order accuracy for the hyperbolic problem, the boundary points must be closed with at least fifth-order formulas, which for the optimal schemes the short hand nomenclature would be (5,5-6-5,5). (Again, note that there is no ambiguity in comparing this nomenclature with that from the sixth-order explicit scheme, since it would require three boundary formulas at each end of the domain.) In keeping with the convention of this work, the closure at each end of the domain is done in a asymmetric manner, so that either the inflow or the outflow problem can be easily accommodated.

It has proven extremely difficult to find G-K-S stable schemes which are formally sixth-order accurate. We, therefore, begin the discussion by presenting the stability analysis of a family of lower-order schemes. Two of the schemes in this family are the 1) (3,5-6-5,3) and 2) (4,5-6-5,4). The formal accuracies of these schemes are fourth- and fifth-order, respectively. The closure at the grid-point j=0 (with corresponding formulas written at j=N) is accomplished by

$$\frac{\partial U_0}{\partial x} + 2\frac{\partial U_1}{\partial x} = \frac{-5U_0 + 4U_1 + U_2}{2\Delta x} \tag{93}$$

$$\frac{\partial U_0}{\partial x} + 3\frac{\partial U_1}{\partial x} = \frac{-17U_0 + 9U_1 + 9U_2 - U_3}{6\Delta x} \tag{94}$$

for the third- and fourth-order schemes, respectively, while the fifth-order closure at the point next to the wall is accomplished in all cases by the scheme

$$\frac{\partial U_0}{\partial x} + 6\frac{\partial U_1}{\partial x} + 3\frac{\partial U_2}{\partial x} = \frac{-10U_0 - 9U_1 + 18U_2 + U_3}{3\Delta x}. \tag{95}$$

Wider spatial stencils produce stability polynomials of dramatically increased complexity. Despite the fact that MACSYMA was used to determine all of the spatial formulas and the stability polynomial of the sixth-order schemes, the possibility for error still exists. Noting the ability of the G-K-S theory to accurately predict the stability envelop of the one-parameter family of fourth-order compact schemes (1^1-4-4), a simple test was devised to verify the accuracy of the G-K-S calculations. A one-parameter family of schemes was created by combining the third- and fourth-order closure formula at each end of the domain. Symbolically, the combined scheme is represented by (3^1,5-6-5,3^1), and is written as

$$\alpha[\frac{\partial U_0}{\partial x} + 2\frac{\partial U_1}{\partial x} - \frac{-5U_0 + 4U_1 + U_2}{2\Delta x}] + (1-\alpha)[\frac{\partial U_0}{\partial x} + 3\frac{\partial U_1}{\partial x} - \frac{-17U_0 + 9U_1 + 9U_2 - U_3}{6\Delta x}] = 0. \tag{96}$$

For $\alpha = 0$ (or 1), the scheme produces the optimal fourth-order (or third-order) variant, and for all other values of α, the formula is a third-order scheme.

The model equation for the outflow quarter-plane problem is the same as described in eqn (83). Solutions of the form $U_j(t) = \exp^{St}\phi_0\kappa^j$, satisfy the numerical scheme, giving the sixth-order inner-scheme the resolvent condition

$$(\frac{1}{\kappa} + 3 + \kappa)\hat{S} = (-\frac{1}{\kappa^2} - \frac{28}{\kappa} + 28\kappa + \kappa^2)/12 \tag{97}$$

for the eigenvalue $\hat{S}$. There are, in general, two roots to the resolvent equation which will yield $|\kappa| < 1$ for large $\mathcal{R}(\hat{S})$, since the resolvent is a polynomial of degree four. The other two roots will become exponentially unbounded as j becomes large and can be ignored. The general solution has the form $U_j(t) = \exp^{St}(C_1{\kappa_1}^j + C_2{\kappa_2}^j)$. Substituting this expression into the boundary eqns (95,97) yields expressions for the constants C_1 and C_2. The expressions are

$$\begin{aligned} C_1F_0(\kappa_1) + C_2F_0(\kappa_2) &= 0 \\ C_1F_1(\kappa_1) + C_2F_1(\kappa_2) &= 0 \end{aligned} \tag{98}$$

where

$$\begin{aligned} F_0(\kappa) &= ((-(6\alpha+18)\kappa - 18\kappa^2)\hat{S} - ((2\alpha+3) + (3\alpha+27)\kappa - (6\alpha+27)\kappa^2 + (\alpha-3)\kappa^3)) \\ F_1(\kappa) &= ((1 + 6\kappa + 3\kappa^2)\hat{S} - (-10 - 9\kappa + 18\kappa^2 + 1\kappa^3)/3). \end{aligned} \tag{99}$$

Equation (98) has only the trivial solution unless the determinant condition $F_0(\kappa_1)F_1(\kappa_2) - F_1(\kappa_2)F_0(\kappa_1) = 0$ is satisfied. Solving the resolvent eqn (97) for $\hat{S}$ and substituting into the determinant condition yields an expression relating the two κ's as

$$(\kappa_1 - 1)^3(\kappa_2 - 1)^3((7\alpha - 3)\kappa_1\kappa_2 + (-2\alpha + 3)(\kappa_1 + \kappa_2) - 3\alpha - 3) = 0. \tag{100}$$

Solving eqn (100) yields $\kappa_1 = 1$ or $\kappa_2 = 1$, or

$$\kappa_1 = \frac{(2\alpha - 3)\kappa_2 + 3\alpha + 3}{(7\alpha - 3)\kappa_2 - 2\alpha + 3}. \tag{101}$$

To obtain an additional independent relationship for κ_1 and κ_2, the resolvent condition eqn (97) is used. Solving the resolvent equation for $\hat{S}$ and noting that both κ_1 and κ_2 satisfy this expression for $\hat{S}$, yields

$$\hat{S} = \frac{(-\frac{1}{{\kappa_1}^2} - \frac{28}{\kappa_1} + 28\kappa_1 + {\kappa_1}^2)}{12(\frac{1}{\kappa_1} + 3 + \kappa_1)} = \frac{(-\frac{1}{{\kappa_2}^2} - \frac{28}{\kappa_2} + 28\kappa_2 + {\kappa_2}^2)}{12(\frac{1}{\kappa_2} + 3 + \kappa_2)}. \tag{102}$$

Combining eqn (101) and eqn (102) produces a single sixth-order polynomial in κ_2, for which the roots can be found numerically. Equation (101) and eqn (97) are then used to determine the numerical values of κ_1 and $\hat{S}$. An eigensolution exists for the problem if, for $|\kappa_1| < 1$ and $|\kappa_2| < 1$, there exists a $\hat{S}$ with real part greater than zero. Solving the outflow polynomial for κ_2 yields the result that the boundary is unstable for $-9.16 < \alpha < -1.86$. The two limiting cases ($\alpha = 0$ and $\alpha = 1$) for which the scheme is fourth- or third-order accurate, are stable. It should be noted that the possibility of instability also exists for the case $\kappa_1 = \kappa_2$, and for κ_1 or $\kappa_2 = 1$. None of these conditions showed instability, however.

The model equation for the inflow quarter-plane problem is the same as described in eqns (87,88). Solutions of the form $U_j(t) = \exp^{St} \phi_0 \kappa^j$, will satisfy the numerical scheme, giving the sixth-order inner-scheme the resolvent condition

$$(\frac{1}{\kappa} + 3 + \kappa)\hat{S} = -(-\frac{1}{\kappa^2} - \frac{28}{\kappa} + 28\kappa + \kappa^2)/12. \tag{103}$$

Eliminating $\frac{\partial U_0}{\partial x}$ between the boundary schemes at grid-points j=0 and j=1, yields an expression written for grid-point j=1 of the form

$$\begin{aligned}(6\alpha + 18)\frac{\partial U_1}{\partial x} + 18\frac{\partial U_2}{\partial x} &= ((2\alpha + 3)U_0 + (3\alpha + 27)U_1 - (6\alpha + 27)U_1 \\ &\quad +(\alpha - 3)U_3))/(6\Delta x).\end{aligned} \tag{104}$$

The general solution has the form $U_j(t) = \exp^{St}(C_1{\kappa_1}^j + C_2{\kappa_2}^j)$. Substituting this expression into the boundary expressions at j=1,2 yields two expressions for the constants C_1 and C_2. The expressions are

$$\begin{aligned}C_1F_1(\kappa_1) + C_2F_1(\kappa_2) &= 0 \\ C_1F_2(\kappa_1) + C_2F_2(\kappa_2) &= 0\end{aligned} \tag{105}$$

where

$$\begin{aligned}F_1(\kappa) &= ((-(6\alpha + 18)\kappa - 18\kappa^2)\hat{S} - (+(3\alpha + 27)\kappa - (6\alpha + 27)\kappa^2 + (\alpha - 3)\kappa^3)) \\ F_2(\kappa) &= 1.\end{aligned} \tag{106}$$

The simple form of the expression $F_2 = 1$ results from reducing the modal equation at point j=2 (with U_0 set to zero) by use of the resolvent condition (with U_0 not equal to zero). Equation (105) can only have a nontrivial solution if the determinant is identically zero. Solving eqn (103) for $\hat{S}$ and substituting into the determinant condition from eqn (105) yields

$$\frac{(2\alpha - 3){\kappa_1}^5 + (-5\alpha + 15){\kappa_1}^4 - 30{\kappa_1}^3 + (6\alpha + 24){\kappa_1}^2 + (-22\alpha - 33){\kappa_1}^1 - (\alpha + 3)}{2{\kappa_1}^2 + 6{\kappa_1}^1 + 2} \quad -$$

$$\frac{(2\alpha-3)\kappa_2{}^5+(-5\alpha+15)\kappa_2{}^4-30\kappa_2{}^3+(6\alpha+24)\kappa_2{}^2+(-22\alpha-33)\kappa_2{}^1-(\alpha+3)}{2\kappa_2{}^2+6\kappa_2{}^1+2} = 0. \tag{107}$$

Together with eqn (102), they provide two equations for the unknown κ_1 and κ_2.

The inflow polynomial equations are far more difficult to solve since they do not factor appreciably. A change of variables from κ_1 and κ_2 to "x" and "y", simplifies the algebra. Substituting

$$\begin{aligned} \kappa_1+\kappa_2 &= 2y \\ \kappa_1\kappa_2 &= x \end{aligned} \tag{108}$$

into eqn (102) yields

$$(-8x-8)y^2+(-12x^2-224x-12)y-2x^3-166x^2-166x-2=0 \tag{109}$$

which has the solution

$$y=\frac{-(3x^3+56x+3\pm\sqrt{5x^4+2490x^2+5})}{4x+4} \tag{110}$$

for $x \neq -1$. (The case x = -1 degenerates into y=0, for which $\kappa_1 = -\kappa_2 = \pm 1$, a condition which produces no eigensolutions). Either root can be used since the final polynomial results from squaring an intermediate result to clear the square root in the expression. Substituting eqn (108) into eqn (107) and further simplifying with the expression for y from eqn (110) yields a ninth-order polynomial in the variable x, with coefficients that are functions of the variable α. Solving this expression numerically yields the roots for x. The values of y are then determined from eqn (110) and the values of κ_1 and κ_2 are obtained from eqn (108). Again, the condition $\kappa = 1$ and the case $\kappa_1 = \kappa_2$ did not show instability over the parameter range tested in this study. For the inflow boundary condition, the instability envelop for the parameter α was determined to be $-1.86 \leq \alpha \leq -0.447$. It is evident that the two degenerate conditions, $\alpha = 0$ and $\alpha = 1$, are G-K-S stable for the inflow. By combining the inflow and outflow results, the theoretical (G-K-S) range of instability for the one-parameter family of schemes (3^1,5-6-5,3^1), was determined to be $-9.18 \leq \alpha \leq -0.447$. The two degenerate cases, (3,5-6-5,3) and (4,5-6-5,4), were both G-K-S stable schemes.

To determine the accuracy of the G-K-S calculations, another method of showing stability was used, and the results were compared. The necessary condition for stability on the eigenvalue structure $\mathcal{R}(S_{max})$ provides such a test. Figure (10) shows the results of an eigenvalue determination spanning the range $-10 \leq \alpha \leq 2$, as determined numerically. The

maximum eigenvalue $\mathcal{R}(S_{max})$ (the eigenvalue with the largest absolute real component), is plotted as a function of the parameter α for three grid densities. Since Lax stability in a finite domain requires that $\mathcal{R}(S) \leq \omega$ for $\omega \geq 0$, the $\mathcal{R}(S_{max})$ should remain bounded with increasing grid density if the scheme is to be stable for a particular value of α. It is apparent from Figure (10), that the stability boundary at $\alpha = -9.15$ is accurately predicted by G-K-S theory. The stability boundary at $\alpha = -0.45$ is less well defined in the eigenvalue determination, and must be further investigated to show the correlation between G-K-S theory and eigenvalue determination. On the relatively coarse grids presented in Figure (10), the maximum eigenvalues near the limit $\alpha = -0.45$ are growing with increasing grid density. Whether they are growing in a bounded manner determines if they satisfy the necessary condition for stability. Table (2) shows the behavior of $\mathcal{R}(S_{max})$ for various grid densities at $\alpha = -0.40$.

Grid	$\mathcal{R}(S_{max})$	$\Delta\%$
21	1.000	NA
41	1.250	25
81	1.360	8
161	1.582	16
321	1.704	8
641	1.780	5

Table 2: Grid convergence of $\mathcal{R}(S_{max})$ for $\alpha = -0.40$.

As the number of grid-points becomes larger, the maximum eigenvalue asymptotes to a constant ω, thus a stable condition. Note that the convergence to the asymptotic limit is slow for $\alpha = -0.40$. Similar grid refinement studies at values of α = -0.45 and -0.50 showed linear growth for all grids, thus an unstable condition. Based on a numerically determined eigenvalue determination over the range of $-10 \leq \alpha \leq 2$, the G-K-S theory is accurately predicting the stability envelop. It should be noted that the slow convergence to the asymptotic limit (and the fact that the test is a necessary not sufficient one) makes testing for stability by numerical eigenvalue determination somewhat unreliable. For many non-borderline cases, it does provide an accurate measure of stability.

The eigenvalue determination provides information on the asymptotic stability of the schemes as well. If for all the grids, the $\mathcal{R}(S_{max}) \leq 0$, the scheme is asymptotically stable. For values of the parameter $\alpha \leq -9.15$ and $\alpha \geq 0.4$, eigenvalue determination indicates asymptotic as well as Lax stability of the resulting scheme. Figure (11) shows the eigenvalue spectrum of the (3,5-6-5,3) and (4,5-6-5,4) schemes. It is apparent that both satisfy the necessary condition of Lax stability, and that the (3,5-6-5,3) scheme is asymptotically stable. Because of the eigenvalues in the RH-P, the (4,5-6-5,4) scheme does not exhibit asymptotic

stability. Figure (12) shows a plot of the error of the solution to the scalar wave equation defined by eqns (28, 29, 30) when discretized with the (4,5-6-5,4) scheme. The time interval was $0 \leq t \leq 100$, and time was advanced with a fourth-order Runge-Kutta scheme. The $\log_{10}$ of the L_2 error is plotted as a function of time for three grid densities: 21, 41, and 81 points, respectively. For a CFL = 1, the error does not grow in time. For CFL's of order 0.1, the error is nearly uniform for a period of time, then begins to grow exponentially with time. In all cases, doubling the grid decreases the error of the simulation by a factor of 16 - 32 (error is dominated by either the fourth-order time, or the fifth-order space truncation terms.) The amplification is accurately predicted by the eigenvalue determination. Table (3) shows the numerical amplification rate compared with the $\mathcal{R}(S_{max})$, for which the agreement is excellent.

Grid	$\alpha_{Numerical}$	$\alpha_{\mathcal{R}(S_{max})}$
21	0.1245	0.1228
41	0.1402	0.1381
81	0.1351	0.1354

Table 3: Numerical vs. Theoretical Growth Rate; (4,5-6-5,4).

The preceding examples of sixth-order schemes show the strength of G-K-S analysis to accurately predict the stability of complex higher-order schemes. They also show the intimate relationship between the eigenvalues of the spatial operator and the stability of the resulting scheme.

We now present schemes that are formally sixth-order accurate, being closed at the boundaries by at least fifth-order stencils. Our first attempt is with optimal fifth-order closure at the boundaries, resulting in the scheme (5,5-6-5,5). Figure (13) shows the error of the simulation of the scalar wave equation defined by eqns (28, 29, 30). The behavior of this scheme is fundamentally different from the (4,5-6-5,4) scheme in several ways. On all grids, the error is always monotonically increasing in time. For CFL's near the theoretical maximum value, the error increases at a lower rate, but is not suppressed as it was with the lower-order schemes. In addition, the exponential growth rate of the error increases with increasing grid density. On the grids shown, the error in the solution could not be systematically reduced by refining the grid and repeating the calculation to a specified time level T. In spite of these differences, the eigenvalue determination still accurately predicts the growth of the solution. Table (4) shows a comparison of the numerical and theoretical amplification rates. The theoretical values are determined from the $\mathcal{R}(S_{max})$ for each grid.

Grid	$\alpha_{Numerical}$	$\alpha_{\mathcal{R}(S_{max})}$
21	0.7121	0.7138
41	1.104	1.010
81	1.749	1.742

Table 4: Numerical vs. Theoretical Growth Rate; (5,5-6-5,5).

Again, the agreement is excellent. The solution grows at a rate which for long times is dominated by the eigenvalue with the maximum real part. The eigenvalue determination accurately predicts the behavior of the numerical solution even for this case which appears not to be Lax stable.

Figure (14) shows a plot of the eigenvalue spectrum for the (5,5-6-5,5) scheme on a 21, 41 and 81 grid. The $\mathcal{R}(S_{max})$ is obviously increasing for these grids, and appears to be increasing without bound, as opposed to an asymptotic limit. This would violate a necessary condition for Lax stability. As was seen in the (3^1,5-6-5,3^1) example, one cannot draw a precise conclusion from grid refined eigenvalue determination, although, the trends have in the cases presented thus far been the same. We must ultimately rely on G-K-S stability theory for the final answer as to whether the scheme is stable.

We begin by determining the stability of the outflow boundary for the (5,5-6-5,5) scheme. The quarter-plane problem appropriate for this analysis is that described in eqn (83). No boundary conditions are necessary, but NBS's are used at grid-points j=0,1. The closure at grid-point 0 is accomplished with

$$\frac{\partial U_0}{\partial x} + 4\frac{\partial U_1}{\partial x} = \frac{-37U_0 + 8U_1 + 36U_2 - 8U_3 + U_4}{12\Delta x} \tag{111}$$

while that of grid-point j=1 is accomplished with eqn (95). Solutions of the form $U_j(t) = \exp^{St}\phi_0\kappa^j$, will satisfy the numerical scheme, giving the sixth-order inner-scheme the resolvent condition shown in eqn (97). There will be two roots to the fourth-order polynomial in κ which are $|\kappa| \leq 1$, and the general solution will have the form $U_j(t) = \exp^{St}(C_1{\kappa_1}^j + C_2{\kappa_2}^j)$. Substituting this expression into the two boundary conditions yields boundary expressions for the constants C_1 and C_2 of the form

$$\begin{aligned} C_1F_0(\kappa_1) + C_2F_0(\kappa_2) &= 0 \\ C_1F_1(\kappa_1) + C_2F_1(\kappa_2) &= 0 \end{aligned} \tag{112}$$

where

$$\begin{aligned} F_0(\kappa) &= ((1+4\kappa_1)\hat{S} - (-37 + 8\kappa + 36\kappa^2 - 8\kappa^3 + \kappa^4)/12) \\ F_1(\kappa) &= ((1+6\kappa+3\kappa^2)\hat{S} - (-10 - 9\kappa + 18\kappa^2 + \kappa^3)/3). \end{aligned} \tag{113}$$

Equation (112) can only have a nontrivial solution if the determinant condition $F_0(\kappa_1)F_1(\kappa_2) - F_1(\kappa_2)F_0(\kappa_1) = 0$ is satisfied. Solving the resolvent condition eqn(97) for $\hat{S}$ and substituting into the determinant condition produces

$$\frac{(\kappa_1-1)^4(\kappa_2-1)^4(\kappa_2-\kappa_1)(4\kappa_2\kappa_1+\kappa_2+\kappa_1-6)}{144\kappa_1\kappa_2({\kappa_1}^2+3\kappa_1+1)({\kappa_2}^2+3\kappa_2+1)} = 0. \tag{114}$$

Solving eqn (114) yields $\kappa_1 = 1$ or $\kappa_2 = 1$, or $\kappa_1 = \kappa_2$, or the expression

$$\kappa_1 = -\frac{\kappa_2 - 6}{4\kappa_2 + 1}. \tag{115}$$

The first two roots are the same roots that have been shown previously to be stable. The condition that both roots must be $|\kappa| \leq 1$ precludes the last root. The third root can be shown to be stable by testing the derivative condition of the polynomial as follows. Multiplying and dividing eqn (112) by the non-zero rows and columns does not change the roots of the determinant conditions. The resulting expression is

$$\begin{vmatrix} F_0(\kappa_1) & \dfrac{F_0(\kappa_2)-F_0(\kappa_1)}{\kappa_2-\kappa_1} \\ F_1(\kappa_1) & \dfrac{F_1(\kappa_2)-F_1(\kappa_1)}{\kappa_2-\kappa_1} \end{vmatrix} = 0.$$

Taking the limit as $\kappa_1 \rightarrow \kappa_2$ yields the expression for the determinant condition $F_0(\kappa)\frac{dF_1(\kappa)}{d\kappa} - F_1(\kappa)\frac{dF_0(\kappa)}{d\kappa} = 0$. The resulting expression for κ is

$$\frac{(\kappa-1)^{12}}{144\kappa^2(\kappa^2+3\kappa+1)^2} = 0. \tag{116}$$

The outflow boundary is, thus, stable for the (5,5-6-5,5) scheme.

The model equation for the inflow quarter-plane problem is the same as described in eqn (87, 88). Solutions of the form $U_j(t) = \exp^{St}\phi_0\kappa^j$, will satisfy the numerical scheme, giving the sixth-order inner-scheme the same resolvent condition as was given in eqn (103). Again, the general solution will have the form $U_j(t) = \exp^{St}(C_1{\kappa_1}^j + C_2{\kappa_2}^j)$. Substituting this expression into the two boundary conditions and making the simplification that $U_0 = 0$ gives two equations for the constants C_1 and C_2 of the form

$$\begin{aligned} C_1F_1(\kappa_1) + C_2F_1(\kappa_2) &= 0 \\ C_1F_2(\kappa_1) + C_2F_2(\kappa_2) &= 0 \end{aligned} \tag{117}$$

where

$$\begin{aligned} F_1(\kappa) &= ((2\kappa+3\kappa^2)\hat{S} - (+44\kappa - 36\kappa^2 - 12\kappa^3 + \kappa^4)/12 \\ F_2(\kappa) &= 1. \end{aligned} \tag{118}$$

The determinant condition for which there is a nontrivial solution simplifies to $F_1(\kappa_1) - F_1(\kappa_2) = 0$ and, along with eqn (102), provide two equations for the two unknowns κ_1 and κ_2. Using the change of variables $\kappa_1 + \kappa_2 = 2y$ and $\kappa_1\kappa_2 = x$, eqn (118) becomes

$$-64y^5 + (192 - 96x)y^4 + (-16x^2 + 352x - 240)y^3 + (120x^2 - 504x + 160)y^2$$

$$+(8x^3 - 216x^2 + 360x - 56)y - 18x^3 + 142x^2 - 142x + 18 = 0. \quad (119)$$

Substituting the functional relationship y=y(x) provided by eqn (110) into eqn (119) and simplifying yields

$$(x-1)(x+1)^5(x^{12} + 261x^{11} + 24298x^{10} + 864903x^9 + 864903x^9 + 5558711x^8$$

$$+16502410x^7 + 27479264x^6 + 28538822x^5 + 5255107x^4 + 429169x^3$$

$$+ 18614x^2 + 435x + 5) = 0. \quad (120)$$

Two roots to this polynomial give rise to eigenvalues $\hat{S}$ which are in the RH-P. They are $x = (-0.01969168445 \pm 0.02398022319i)$, which yields $\kappa_1 = (0.157055621 \mp 0.943601129i)$, with $\kappa_2 = (-0.02810826491, \mp 0.01619023438i)$ and $\hat{S} = (0.0428389 \pm 1.39944i)$. The numerical solutions satisfy the governing equations to approximately machine precision (1.0e-13). Thus, the inflow for the (5,5-6-5,5) scheme is G-K-S unstable. This verifies the trends presented earlier in the eigenvalue grid refinement analysis, and the simulation of the scalar wave equation, both of which indicated the sixth-order scheme was Lax unstable.

The unstable (5,5-6-5,5) scheme previously discussed was implemented using optimal fifth-order boundary formulas. By relaxing the constraint of optimal order schemes at the boundaries, the possibility of a fifth-order closure which will be G-K-S stable still exists. Taylor series truncation analysis was used to develop parametric relations for the closure formulas at the two NBS's. They were constrained to be fifth-order, and explicit in nature. To facilitate a wide range of closures, each point was given two degrees of freedom. The symbolic formula for the new scheme is, thus, (5^2,5^2-6-5^2,5^2). The scheme defined at grid-point j=0 and 1 can be written as

$$\frac{\partial U_0}{\partial x} = (C_0U_0 + C_1U_1 + C_2U_2 + C_3U_3 + C_4U_4 + C_5U_5 + C_6U_6 + C_7U_7)/(\Delta x) \quad (121)$$

$$\frac{\partial U_1}{\partial x} = (D_0U_0 + D_1U_1 + D_2U_2 + D_3U_3 + D_4U_4 + D_5U_5 + D_6U_6 + D_7U_7)/(\Delta x) \quad (122)$$

where

$$C_0 = -(\alpha_0 - 28\beta_0 + 13068)/5040 \quad (123)$$

$$
\begin{aligned}
C_1 &= +(\alpha_0 - 27\beta_0 + 5040)/720 \\
C_2 &= -(\alpha_0 - 26\beta_0 + 2520)/240 \\
C_3 &= +(\alpha_0 - 25\beta_0 + 1680)/144 \\
C_4 &= -(\alpha_0 - 24\beta_0 + 1260)/144 \\
C_5 &= +(\alpha_0 - 23\beta_0 + 1008)/240 \\
C_6 &= -(\alpha_0 - 22\beta_0 + 840)/720 \\
C_7 &= +(\alpha_0 - 21\beta_0 + 720)/5040
\end{aligned}
$$

and

$$
\begin{aligned}
D_0 &= -(\alpha_1 - 21\beta_1 + 720)/5040 \\
D_1 &= +(\alpha_1 - 20\beta_1 - 1044)/720 \\
D_2 &= -(\alpha_1 - 19\beta_1 - 720)/240 \\
D_3 &= +(\alpha_1 - 18\beta_1 - 360)/144 \\
D_4 &= -(\alpha_1 - 17\beta_1 - 240)/144 \\
D_5 &= +(\alpha_1 - 16\beta_1 - 180)/240 \\
D_6 &= -(\alpha_1 - 15\beta_1 - 144)/720 \\
D_7 &= +(\alpha_1 - 14\beta_1 - 120)/5040
\end{aligned}
\tag{124}
$$

with similar expressions defined for the closure at the other end of the domain. By systematically searching the four-parameter space spanned by the parameters $\alpha_0, \beta_0, \alpha_1$, and β_1 with an eigenvalue code, an arbitrary eigenvalue spectrum can be approximated. A particular set of coefficients for which the eigenvalue spectrum is bounded to the Left Half-Plane is $\alpha_0 = 1809.257, \beta_0 = -65.1944, \alpha_1 = -262.16$ and $\beta_1 = -26.6742$. The values are not unique and no attempt has been made to find optimal values of these coefficients. The eigenvalue spectrum for this case is shown on Figure (14). Note that the shape of the spectrum is similar to that of the (5,5-6-5,5) scheme, but that the $\mathcal{R}(S_{max}) \leq 0$ instead of increasing without bound. The scheme satisfies the necessary condition for Lax stability, and is asymptotically stable by our definitions.

The stability analysis for the two quarter-plane problems involved in establishing the G-K-S stability of the new $(5^2, 5^2\text{-}6\text{-}5^2, 5^2)$ is extremely formidable. It pushes MACSYMA to the limits of its capabilities on present machines. In addition, 128-bit arithmetic is required to ensure precision when determining the roots of the resulting polynomials in "x". The scheme has been shown to be G-K-S stable for the parameters given above for the inflow and outflow problems. Thus a formally sixth-order scheme has been developed which is G-K-S (Lax) stable, and asymptotically stable for the scalar case.

To verify its accuracy, Table (5) shows a grid refinement study performed with the new sixth-order scheme. The model problem is the scalar wave equation defined by eqns (28, 29, 30). The time advancement scheme is the fourth-order Runge-Kutta algorithm, with a CFL of 0.10. Temporal refinement studies were performed to ensures that the leading error terms on all grids were from the spatial discretization operator. Listed is the grid and its error, and the slope between each successive refinement. The asymptotic stability of the spatial operator ensure that the solution does not grow exponentially for long times.

Grid	$L_2 error$	slope
21	-2.363	NA
31	-3.582	-6.9
41	-4.225	-5.1
51	-4.724	-5.1
61	-5.150	-5.4
81	-5.849	-5.6
101	-6.406	-5.7
121	-6.867	-5.8

Table 5: Grid refinement study of the $(5^2, 5^2\text{-}6\text{-}5^2, 5^2)$ scheme.

The data point corresponding to 21 grid-points is erroneous because the grid is too coarse for the scheme to exhibit its higher-order properties. Note that in this example the scheme becomes at least fifth-order accurate at approximately 10 grid-points/(2π radians). In the limit $N \rightarrow \infty$ where N is the number of grid-points, the scheme shows a slope of -6, the formal accuracy of the inner-scheme. Note that for N small, the four points which are treated with fifth-order accuracy degrade the formal accuracy by one degree.

An asymptotically stable sixth-order spatially accurate scheme has been developed for use in a method-of-lines discretization of a hyperbolic partial differential equation. The eigenvalues of the new scheme are for the scalar case bounded to the Left Half-Plane of the complex plane for all N. The necessary condition for Lax stability is, therefore, satisfied. In addition, the scheme has been shown to be G-K-S stable for the combined inflow and outflow quarter-plane analysis, and is, therefore, formally Lax stable for the scalar case. For the hyperbolic system of equations, the use of any of the Lax stable schemes presented in this work guarantees the Lax stability of the resulting spatial discretization if the boundaries are imposed in characteristic form. The concept of asymptotic stability does not carry over from the scalar case to the system. For the case of the system with all of the physical eigenvalues of the same sign, the asymptotic stability is still retained. For the case of mixed eigenvalues, it is easy to show that even though being asymptotically stable for the scalar case, exponential growth of the solution may occur for boundaries that are imposed in characteristic form.

Work continues in this area, to determine a stronger necessary condition for asymptotic stability that will allow the use of scalar analysis to determine spatial schemes which are asymptotically stable for the system.

9. CONCLUSIONS

The stability characteristics of various compact fourth- and sixth-order spatial operators were assessed using the theory of Gustafsson, Kreiss and Sundstrom (G-K-S) for the semi-discrete IBVP. The class of central difference interior schemes with asymmetrically closed boundaries was analyzed. Because of formal accuracy considerations, those schemes with boundary closures of at least $(N-1)^{th}$ spatial order for an $(N)^{th}$ order inner scheme were the focus of the work. It was found that conventional third- or fourth-order boundary conditions, when coupled with the fourth-order compact inner-scheme, resulted in a G-K-S stable scheme. For the sixth-order compact inner-scheme, the conventional boundary closures of fifth- and higher-order were found to be G-K-S unstable. Fourth-order and lower-order closure formulas were found to be G-K-S stable. These results were then generalized to the fully discrete case using a recently developed theory of Kreiss, which states that under weak constraints, the stability of the semi-discrete operator implies stability of the fully discrete operator if a locally stable temporal method is used.

The conventional definition of stability was then sharpened to include only those spatial discretizations that are asymptotically stable (bounded Left Half-Plane eigenvalues). Many of the higher-order schemes which are G-K-S stable were found to not be asymptotically stable. Fourth-order boundary conditions were found to be asymptotically unstable for the schemes, tested, specifically: 1) (4-4-4), and 2) (4,5-6-5,4). A series of compact fourth- and sixth-order schemes which were both asymptotically and G-K-S stable were then developed. The constraint of optimal accuracy from a specific number of constraints was abandoned, thus enabling several-parameter family boundary closures to be developed. A three parameter family uniformly fourth-order scheme (4^3-4-4^3), as well as a four-parameter sixth-order scheme with fifth-order boundaries ($5^2, 5^2$-6-$5^2, 5^2$) were developed which were asymptotically stable. No attempt was made to optimize the parameters.

All the schemes which were found to be G-K-S stable were subjected to extensive comparisons between the G-K-S stability predictions, semi-discrete eigenvalue determination and numerical simulations. In all cases, consistent and complementary results were achieved with all three methods. In addition, it was shown that the eigenvalue determination accurately predicted the exponential divergence of the solution for the cases which were not asymptotically stable. Work continues in developing asymptotic definitions for the case of systems of equations.

References

[1] Kopal, Z., *Numerical Analysis*, 2nd. ed., John Wiley and Sons, 1961.

[2] Vichnevetsky, R., Bowles, J. B., *Fourier Analysis of Numerical Approximations of Hyperbolic Equations*, SIAM, Philadelphia/1982.

[3] Gustafsson, Bertil, "The Convergence Rate for Difference Approximations to Mixed Initial Boundary Value Problems," Math. Comp. **29**, 130 (1975), pp. 396-406.

[4] Osher, S., "Systems of Difference Equations with General Homogeneous Boundary Conditions," Trans. Amer. Math. Soc. **137**, 1969, pp. 177-201.

[5] Kreiss, H.-O., "Initial Boundary Value Problems for Hyperbolic Systems," Comm. Pure Appl. Math. **23**, 1970, pp. 277-298.

[6] Gustafsson, B., Kreiss, H.-O., and Sundstrom, A., "Stability Theory of Difference Approximations for Mixed Initial Boundary Value Problems. II," Math. Comp. **26**, 1972, pp. 649-686.

[7] Trefethen, L.N., "Group Velocity Interpretation of the Stability Theory of Gustafsson, Kreiss, and Sundstrom," J. Comput. Phys. **49**, 1983, pp. 199-217.

[8] Strikwerda, J. C., "Initial Boundary Value Problems for the Method of Lines," J. Comp. Phys. **34**, 1980, pp. 94-107.

[9] Kreiss, H.-O. and Wu. L., "On the Stability Definitions of Difference Approximations for the Initial Boundary Value Problem," Comm. Pure Appl. Math., to appear.

[10] Gottlieb, D., Gunzburger, M., and Turkel, E., "On Numerical Boundary Treatment of Hyperbolic Systems for Finite Difference and Finite Element Methods," SIAM J. Numer. Anal. **19**, 4 (1982).

[11] Gary, J., "On Boundary Conditions for Hyperbolic Difference Schemes," J. Comp. Phys. **26**, 1978, pp. 339-351.

[12] Gear, C. William, *Numerical Initial Value Problems in Ordinary Differential Equations*, Prentice-Hall, Inc., 1971.

[13] Hirsch, Morris W. and Smale, Stephen, *Differential Equations, Dynamical Systems, and Linear Algebra*, Academic Press, Inc., 1974.

[14] Reddy, Satish C. and Trefethen, Lloyd N., "Lax-Stability of Fully Discrete Spectral Methods VIA Stability Regions and Pseudo-Eigenvalues," Proceeding of the ICOSA-HOM'89 Conference, Spectral and High Order Methods For Partial Differential Equations, Publisher, North Holland.

[15] Lele, S.K., "Compact Finite Difference Schemes with Spectral-Like Resolution," Center for Turbulence Research Manuscript 107, April 1990.

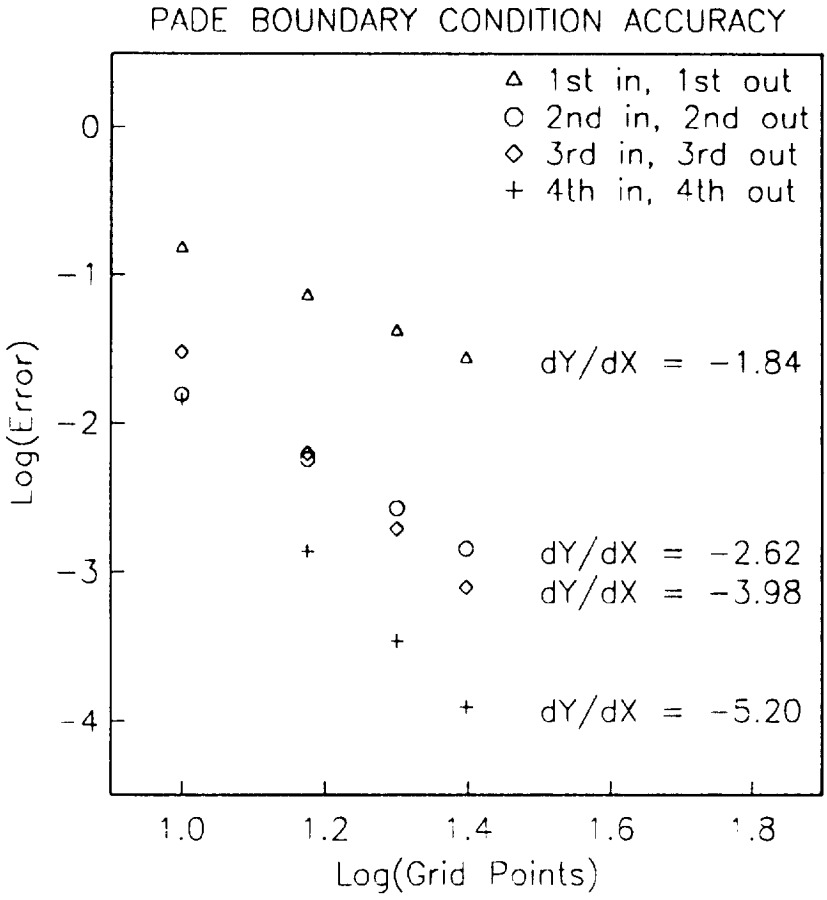

Fig–1 Comparative study of the effects of boundary closure on the formal accuracy of the fourth-order compact inner scheme.

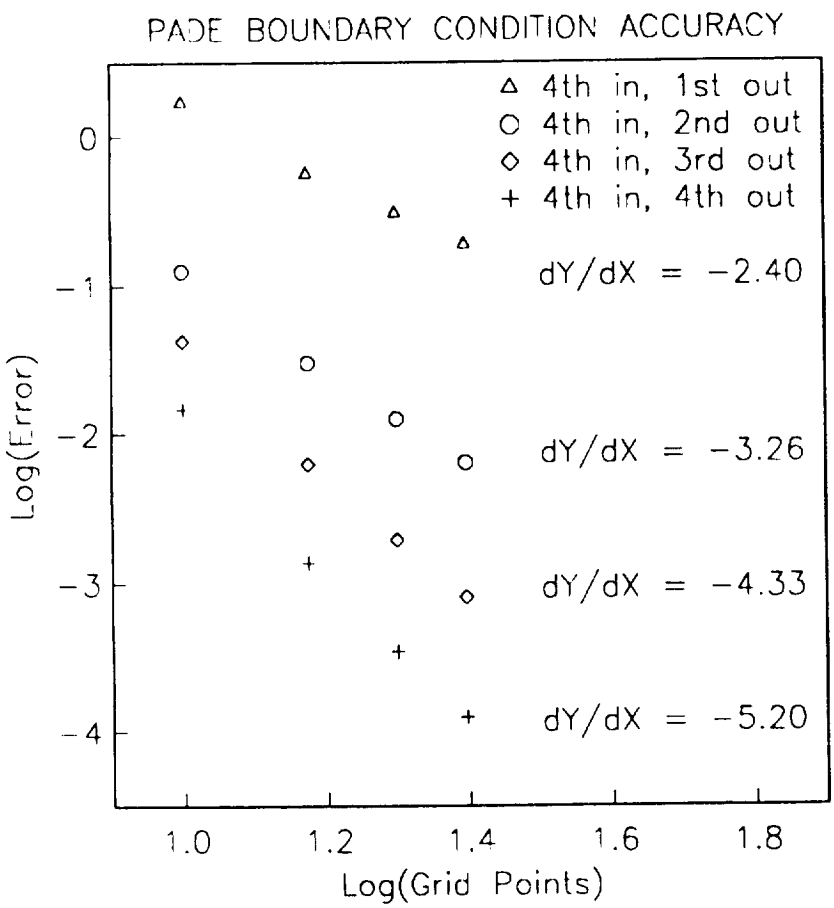

Fig–2 Comparative study of the effects of outflow boundary closure on the formal accuracy of the fourth-order compact inner scheme.

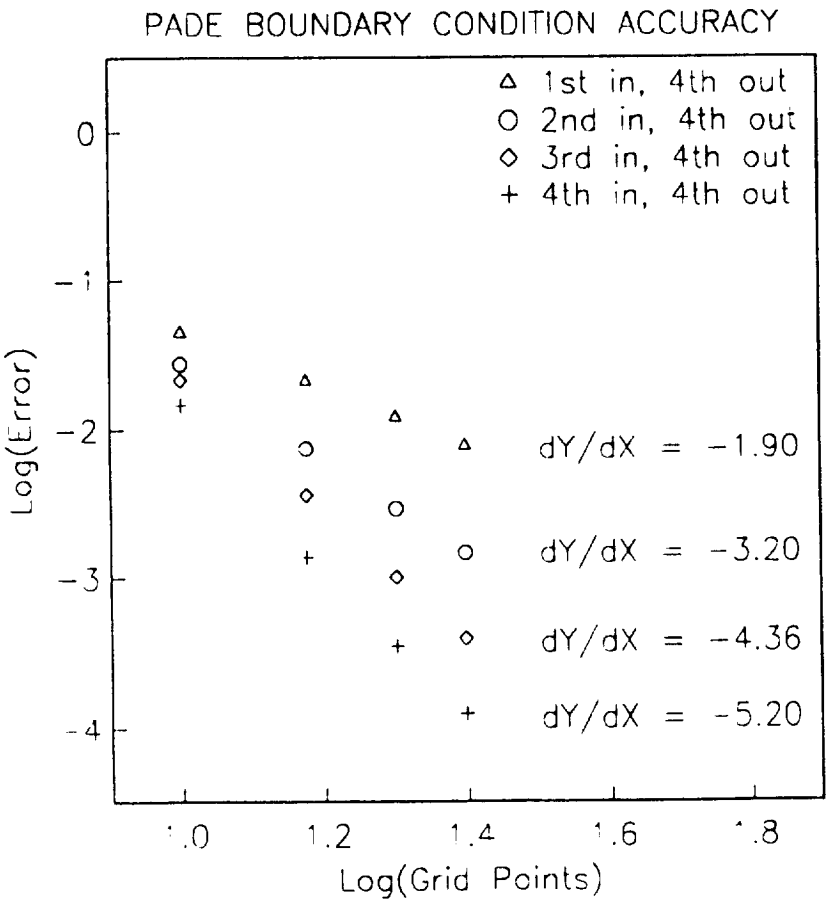

Fig–3 Comparative study of the effects of inflow boundary closure on the formal accuracy of the fourth-order compact inner scheme.

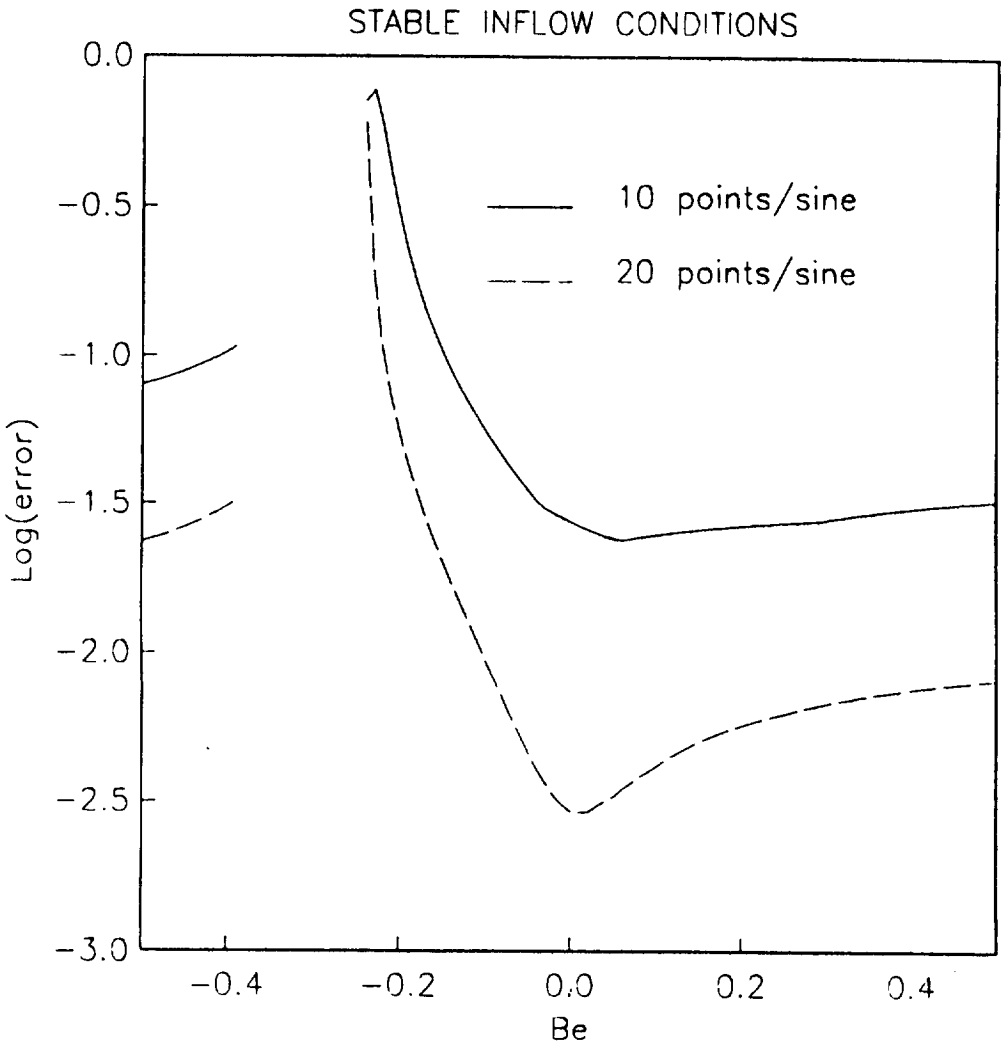

Fig-4 Numerical determination of the L_2 error at a time level "T" resulting from a one-parameter family of closure formulas at the inflow boundary. The inner scheme is the fourth-order Pade scheme.

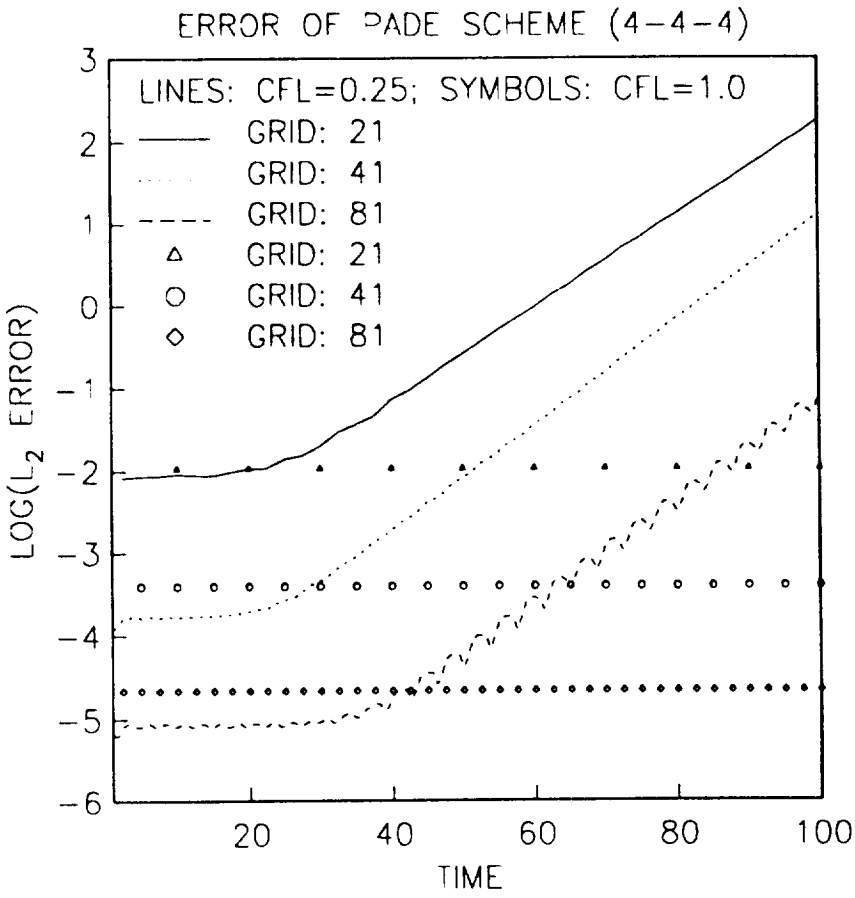

Fig–5 The L_2 error as a function of time, resulting from the uniformly fourth-order Pade scheme (4-4-4), for various CFL's and grid densities.

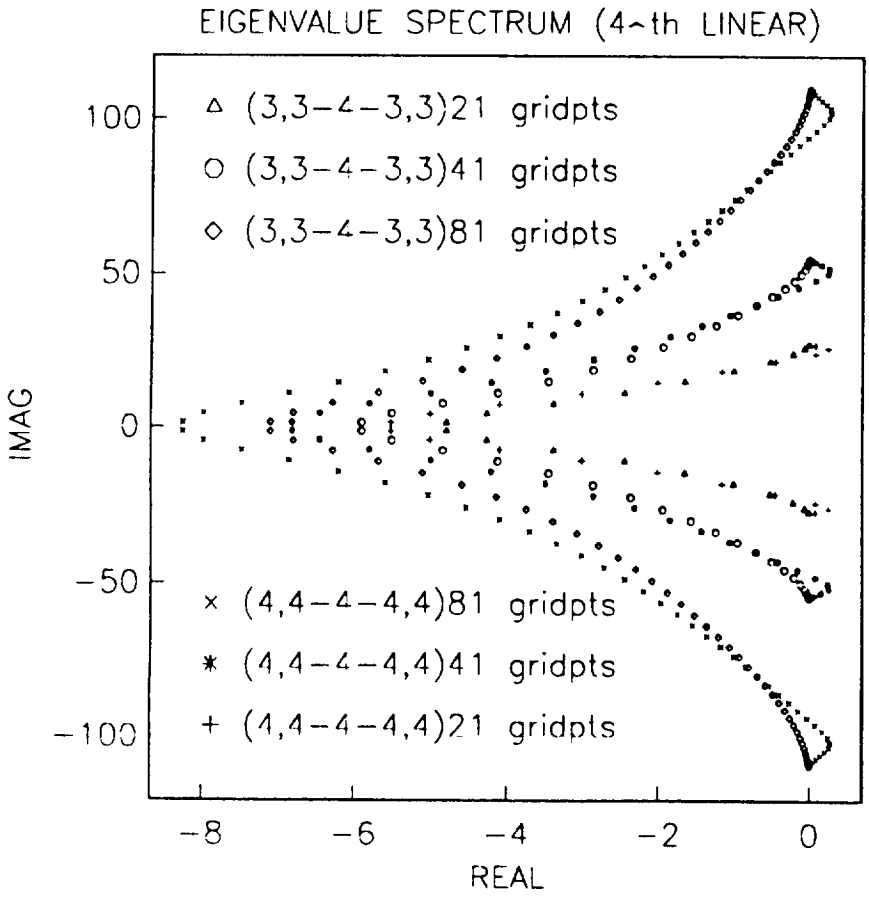

Fig–6 The numerically determined eigenvalue spectrum resulting from the explicit fourth-order inner scheme, closed with either third- or fourth-order boundary schemes.

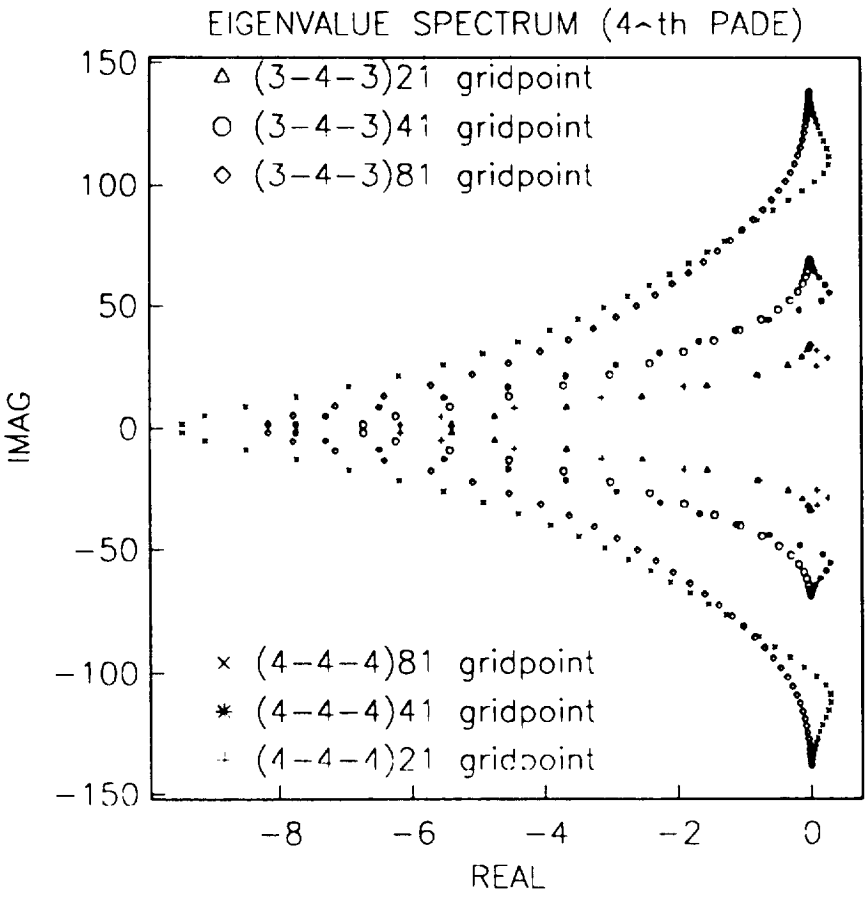

Fig–7 The numerically determined eigenvalue spectrum resulting from the fourth-order Pade inner scheme, closed with either third- or fourth-order boundary schemes.

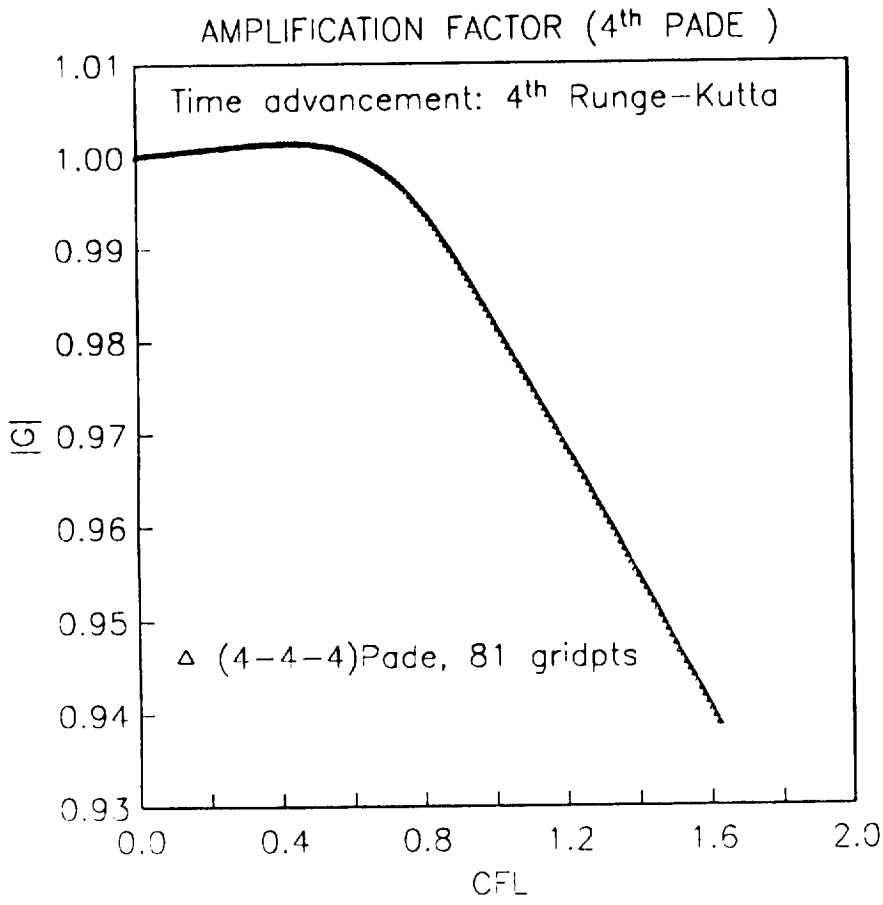

Fig-8 The maximum numerical amplification factor as a function of CFL, plotted for the uniformly fourth-order Pade scheme, with a fourth-order Runge-Kutta time advancement scheme.

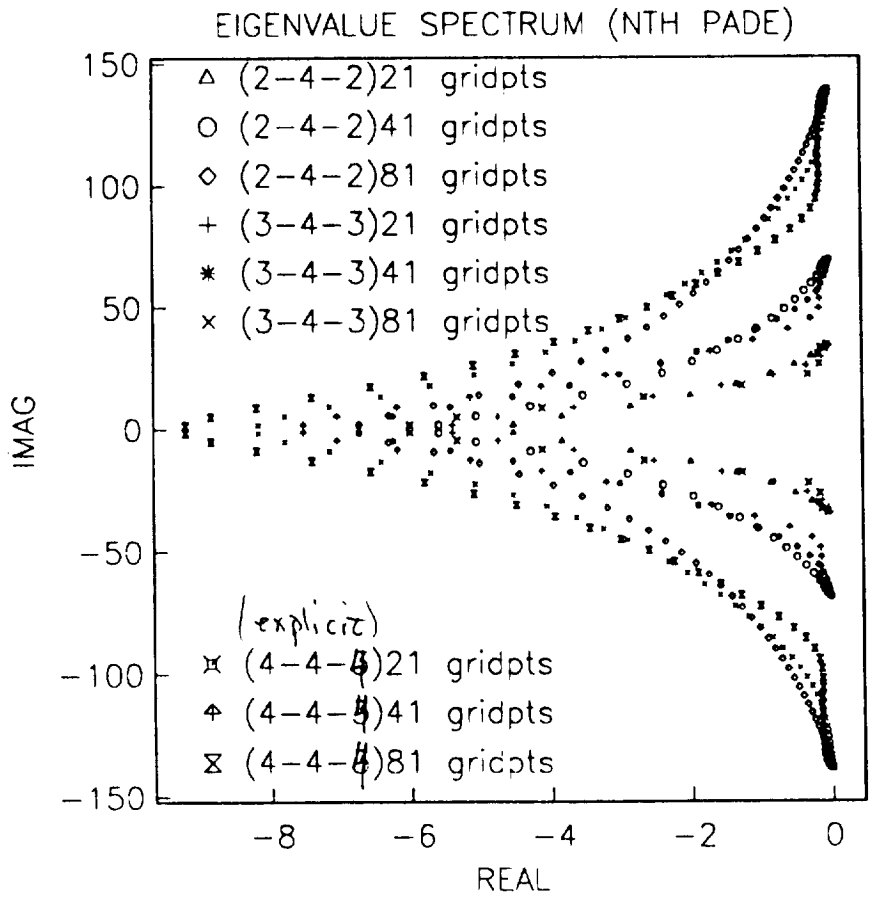

Fig–9 The numerically determined eigenvalue spectrum resulting from the fourth-order Pade inner scheme, closed with either second-, third- or newly developed fourth-order boundary schemes, on various grids.

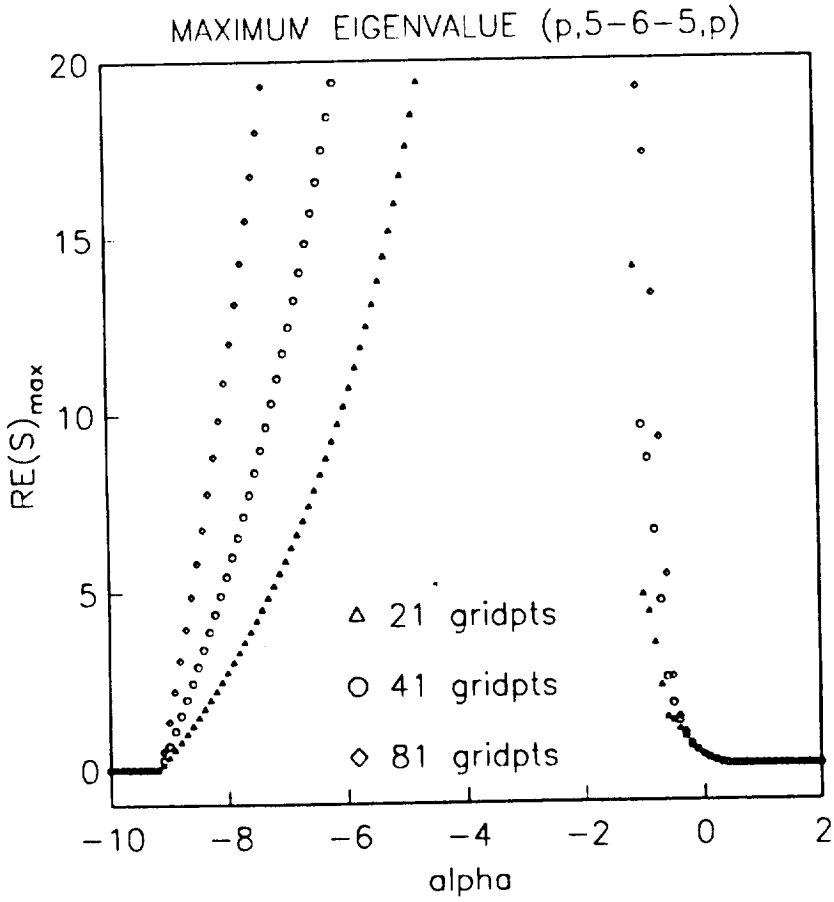

Fig-10 The maximum real part of the numerically determined eigenvalue spectrum, resulting from a sixth-order Pade inner scheme and a one-parameter family of third-order boundary schemes. The ordinant α is the boundary parameter.

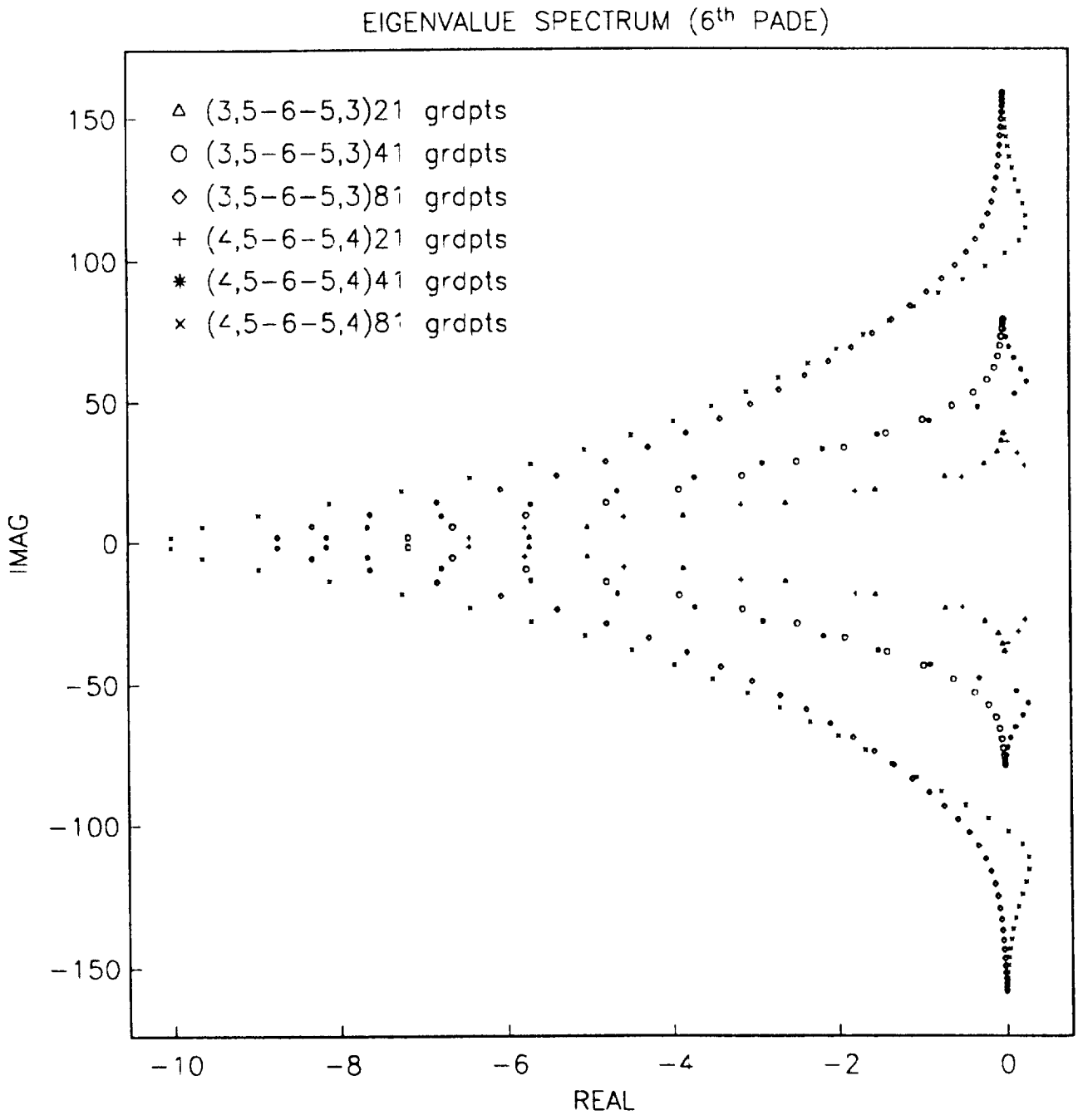

Fig–11 The numerically determined eigenvalue spectrum resulting from the sixth-order Pade inner scheme, closed with either third- or fourth-order boundary schemes, on various grids.

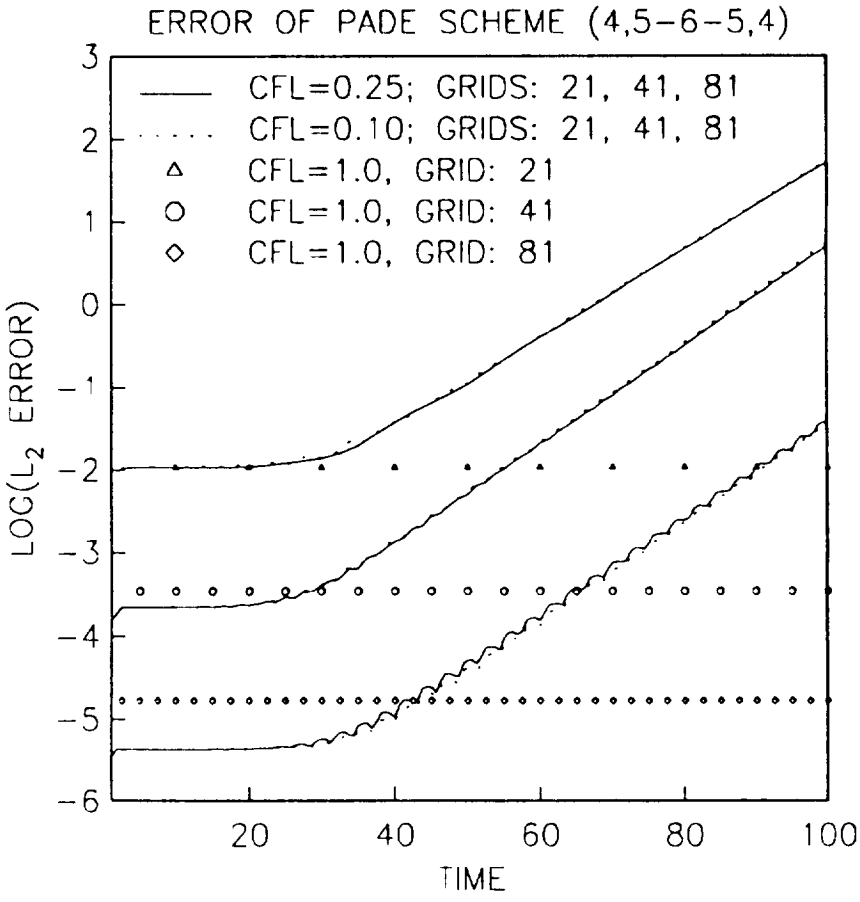

Fig-12 The L_2 error as a function of time, resulting from the uniformly sixth-order Pade scheme with fourth-order boundary closure (4,5-6-5,4), for various CFL's and grid densities.

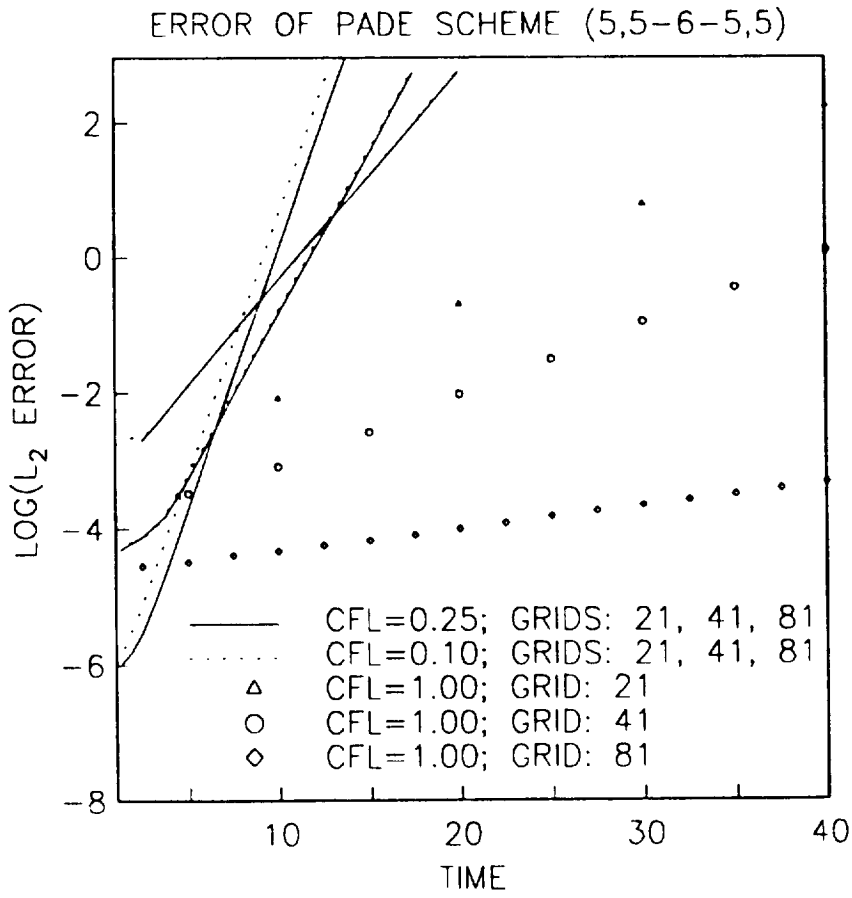

Fig-13 The L_2 error as a function of time, resulting from the uniformly sixth-order Pade scheme with fifth-order boundary closure (5,5-6-5,5), for various CFL's and grid densities.

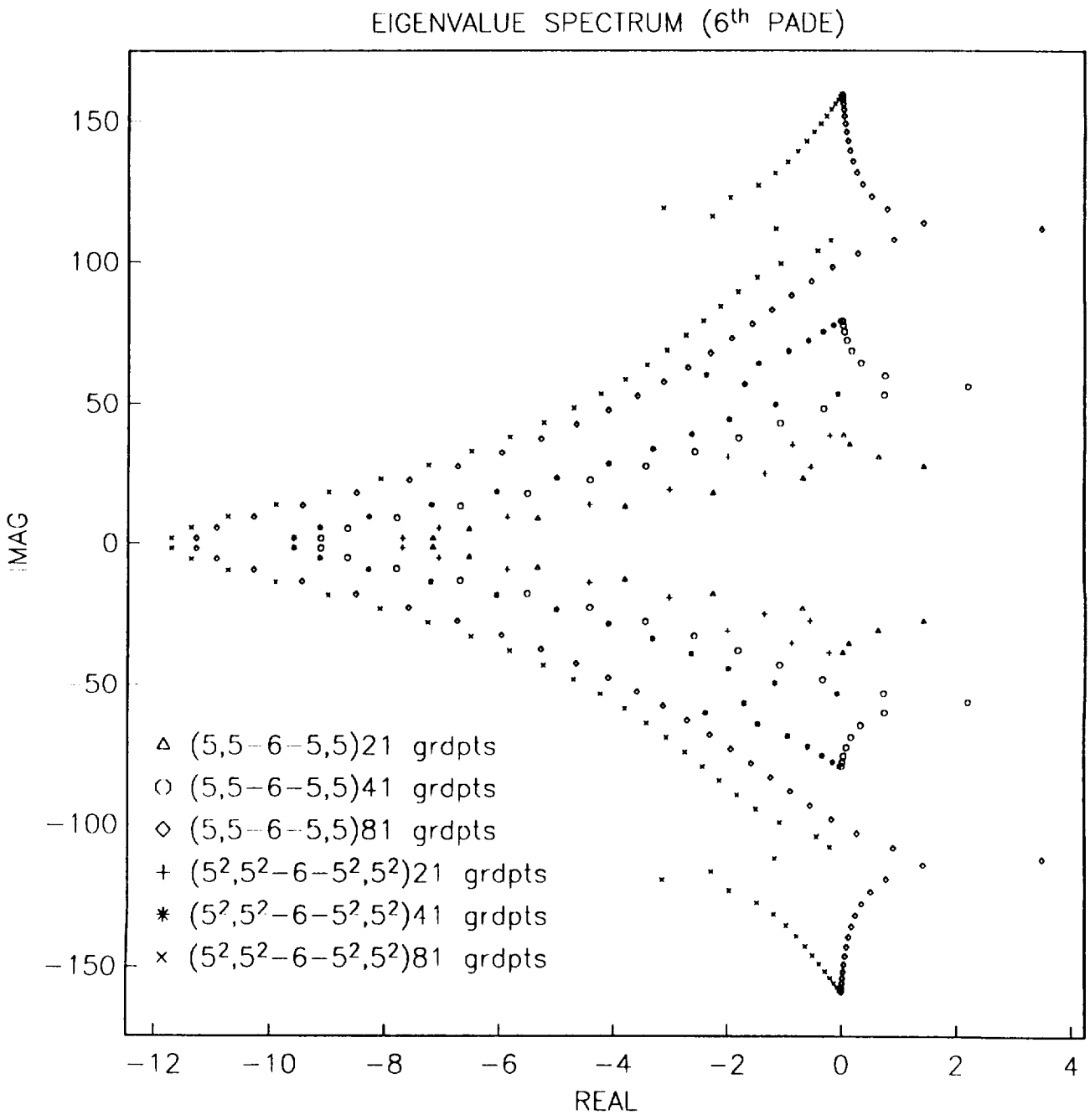

Fig–14 The numerically determined eigenvalue spectrum resulting from the sixth-order Pade inner scheme, closed with conventional fifth- or newly developed fifth-order boundary schemes, on various grids.

NASA
National Aeronautics and Space Administration

Report Documentation Page

1. Report No.	2. Government Accession No.	3. Recipient's Catalog No.
NASA CR-187628 ICASE Report No. 91-71		

4. Title and Subtitle

THE STABILITY OF NUMERICAL BOUNDARY TREATMENTS FOR COMPACT HIGH-ORDER FINITE-DIFFERENCE SCHEMES

5. Report Date

September 1991

6. Performing Organization Code

7. Author(s)

Mark H. Carpenter
David Gottlieb
Saul Abarbanel

8. Performing Organization Report No.

91-71

10. Work Unit No.

505-90-52-01

9. Performing Organization Name and Address

Institute for Computer Applications in Science and Engineering
Mail Stop 132C, NASA Langley Research Center
Hampton, VA 23665-5225

11. Contract or Grant No.

NAS1-18605

13. Type of Report and Period Covered

Contractor Report

12. Sponsoring Agency Name and Address

National Aeronautics and Space Administration
Langley Research Center
Hampton, VA 23665-5225

14. Sponsoring Agency Code

15. Supplementary Notes

Langley Technical Monitor:
Michael F. Card

Final Report

To be submitted to Journal of Computational Physics

16. Abstract

The stability characteristics of various compact fourth- and sixth-order spatial operators are assessed using the theory of Gustafsson, Kreiss and Sundstrom (G-K-S) for the semi-discrete Initial Boundary Value Problem (IBVP). These results are then generalized to the fully discrete case using a recently developed theory of Kreiss. In all cases, favorable comparisons are obtained between G-K-S theory, eigenvalue determination, and numerical simulation. The convential definition of stability is then sharpened to include only those spatial discretizations that are asymptotically stable (bounded, Left Half-Plane eigenvalues). It is shown that many of the higher-order schemes which are G-K-S stable are not asymptotically stable. A series of compact fourth- and sixth-order schemes, which are both asymptotically and G-K-S stable for the scalar case, are then developed.

17. Key Words (Suggested by Author(s))	18. Distribution Statement
compact high order schemes; G-K-S stability; asymptotic stability	64 - Numerical Analysis Unclassified - Unlimited

19. Security Classif. (of this report)	20. Security Classif. (of this page)	21. No. of pages	22. Price
Unclassified	Unclassified	57	A04

NASA FORM 1626 OCT 86

NASA-Langley, 1991